MICROMECHANICAL CHARACTERIZATION OF BRAIN WHITE MATTER WITH BI-DIRECTIONAL ORIENTATION OF AXONAL FIBERS

A Paper
Submitted to the Graduate Faculty
of the
North Dakota State University
of Agriculture and Applied Science

By

Saurav Shankar

In Partial Fulfillment of the Requirements
for the Degree of
MASTER of SCIENCE

Major Department:
Mechanical Engineering

December 2014

Fargo, North Dakota

North Dakota State University

Graduate School

Title

Micromechanical Characterization of Brain White Matter with Bi-directional Orientation of Axonal Fibers

By

Saurav Shankar

The Supervisory Committee certifies that this ***disquisition*** complies with North Dakota State University's regulations and meets the accepted standards for the degree of

MASTER OF SCIENCE

SUPERVISORY COMMITTEE:

Dr. Ghodrat Karami
Chair

Dr. Mariusz Ziejewski

Dr. Fardad Azarmi

Dr. Yildirim Bora Suzen

Dr. Kalpana Katti

Approved:

4/1/2015
Date

Dr. Alan R. Kallmeyer
Department Chair

ABSTRACT

Axonal injury within the white matter of human brain and spinal cord has led to several diseases in the Central Nervous System (Karami and Shankar, [1]). Diffuse axonal injury, one of the forms of Traumatic Brain Injury is caused due to swelling and elongation of axons in case of explosions, small and severe accidents, falling from heights where the brain gets an impact due to sudden movement of skull or hit by an object. A brain tissue model with bidirectional orientation of axonal fibers within the white matter of human brain has been developed. This brain tissue represents a repeating unit cell (RUC) modeled in ABAQUS (finite element software) [2] which comprises of axons and extracellular matrix (Karami and Shankar, [1]). Hyperelastic material properties of white matter sheet *corona radiata* of a porcine brain with bi-directional orientation of axonal fibers within the extracellular matrix is considered (Karami and Shankar, [1]).

ACKNOWLEDGEMENTS

The author would like to acknowledge the Air Force Office of Scientific Research (AFOSR) for the financial support provided for this research work.

I would like to thank my advisor, Dr. Ghodrat Karami for his constant support and encouragement towards my research. My heartfelt gratitude to other committee members:
Dr. Mariusz Ziejewski, Dr. Fardad Azarmi, Dr. Yildirim Bora Suzen and Dr. Kalpana Katti for allocating time in their busy schedules to serve on my committee. My humble regards to my parents who always showed me the right direction, my teachers and my family members. My deepest gratitude to Ushashi and many other friends for their constant support and help.

TABLE OF CONTENTS

LIST OF TABLES

Table Page

LIST OF FIGURES

1. INTRODUCTION TO MULTISCALE BRAIN TISSUE ANALYSIS AND MODELING

1.1. TBI And Diffuse Axonal Injury

Brain is considered as the most complex part of human anatomy and the study regarding brain injury has been a primary focus for many researchers from various fields of science and engineering. Brain injuries due to the road accidents, hit by an external object and sudden head motion due to falling are common these days. It is a major issue in the present world and remains one of the key factors for losing life among children, youths, solders, and workers. There are many factors which result in brain injury but one of the most important aspects is Traumatic brain injury (TBI). The reason for this type of injury can be blasts, falling from heights and in most cases minor or severe road accidents.

Gray matter and white matter form the outer and inner layers of the brain. The inner layer, white matter is composed of fibers known as axonal fibers surrounded by extracellular matrix (Karami and Shankar, [1]). This paper deals with injury caused to inner portion of the brain, the axons which swell or elongate by a fast moving external source developing shearing forces that cause Diffuse axonal injury (Wolf J.A et al. [4]), a type of Traumatic brain injury (Karami and Shankar, [1]). DAI can be caused when the head comes in direct impact with a hard object or an indirect impact e.g. blast wave. Axonal fibers are prone to elongate more in the brain center due to the direct or indirect impact of an object which are eventually injured. Axonal fibers are mainly present in the white matter of the human brain. Human brain is under shearing forces due to the impact. Shear forces developed in the white matter of human brain causes axonal fibers to lengthen and axon injury takes place in microscopic level.

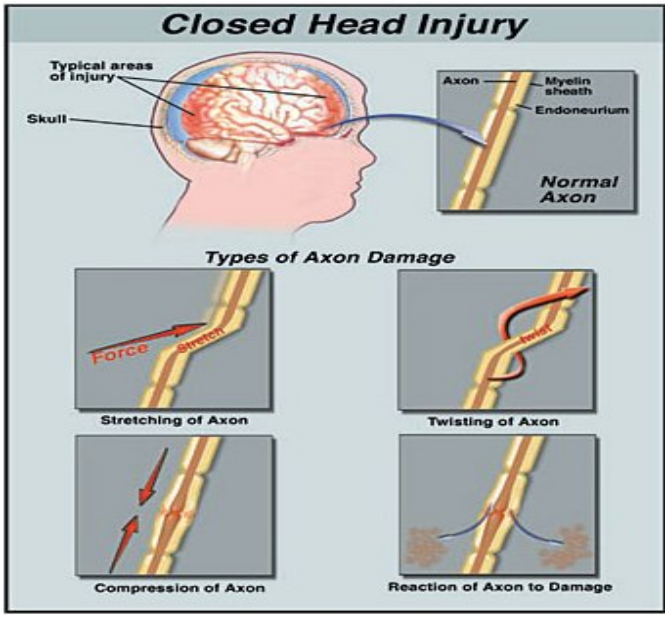

Fig 1. Different types of Axonal Damage (Rhawn Joseph, [3]).

From Fig. 1, it can be seen that how a normal axon is damaged due to application of force which might cause the axon to stretch, twist or compress. In this research, stretching of axons and the damage caused to the white matter sheet *corona radiata* will be examined.

1.2. Relevant Past Works

The orientation of axons within the white matter of the human brain is vague due to brain complexity. Some studies have been performed to understand the brain tissue behavior and orientation of fibrous axons embedded in the extracellular matrix within the white matter of human brain. The axonal fibers embedded within the base matrix are heterogeneous which makes the white matter in the brain behave heterogeneously. In vivo and in vitro test were conducted by many researchers by considering the white matter sheets of the porcine brain and they found experimentally that the *corpus collasum* white matter sheet had a uniaxial orientation of axons while *corona radiata* had a disorder orientation. *Corpus callosum* and *corona radiata* are the white matter sheets where the axonal fibers are majorly located and which have been a

prime focus in biomechanical research field for traumatic brain injury. There have been several attempts to model the orientation of axons distributed in the extracellular matrix within the white matter of brain tissue (Karami and Shankar, [1]). Work has been done for hexagonal and square arrangement of axons spread in a unidirectional orientation within the extracellular matrix but little has been mentioned about the bi-directional distribution of axonal fibers. The reason for modeling crossed axonal fibers within the base matrix is because the white matter sheet *corona radiata* has a disordered pattern of axons as mentioned by Velardi et al. [5], (Karami and Shankar, [1]). The researchers have always focused on the white matter sheet *corpus collasum* with uniaxial orientation of axons for developing brain tissue models but bi-directional arrangement of axons in *corona radiata* still remains unexplored (Karami and Shankar, [1]). Arbogast and Marguiles [6] reported that the ideal axonal fiber volume fraction was 53%, the direction of axonal fibers within the extracellular matrix were uniaxial, and even concluded that fiber is three times stiffer than the matrix.

In developing computational models for axons oriented within the white matter of the brain tissue, hexagonal arrangement of axonal fibers within the extracellular matrix with unidirectional pattern of axons having viscoelastic and hyper-elastic material properties were considered by Abolfathi et al. [7] and Karami et al. [8]. *Corona radiata* is the white matter sheet which is believed to have a bidirectional orientation of axons is an area in the field of biomechanics which remains unexplored by the researchers. Hyper-elastic material for axons and base matrix will be used for corona radiata as biological brain tissues are said to have similar properties with that of rubber like material. Here the white matter sheet *corona radiata* is considered as there is a disorder arrangement of axons in the longitudinal and transverse directions when compared to Corpus callosum where there is a uniaxial pattern of axons.

Experimental works conducted by Prange and Margulies (2002) [9] and Velardi et al. [5] on the porcine brain tissue for white matter sheets *corpus collasum* and *corona radiata* has been noteworthy but there has been little work which describes the stresses developed on axons as well as the overall brain tissue for a crossed fiber orientation due to brain injury caused by external forces. (Karami and Shankar, [1])

The exact material properties of brain tissue are difficult to find and hence a lot of research is done in this area. There were experiments conducted by Velardi et al. [5] on porcine brain tissues which have properties similar to brain tissue of humans (Karami and Shankar, [1]). Though there have been experimental works conducted on corona radiata by Velardi et al. [5] but the computational brain tissue models are yet to be developed. To understand the non-linearity and anisotropic characteristic of the brain tissue undergoing large deformations, hyper-elastic material has been used. A repeating unit cell (RUC) is modeled using finite element software-Abaqus (Karami and Shankar, [1]). The RUC consists of axonal fibers within the base matrix having a bi-directional orientation (Karami and Shankar, [1]). Axial loads as well as shear loads are applied on the unit cell representing the brain tissue and hence the maximum, average normal stresses within the entire brain tissue as well as axons and the extracellular matrix are obtained (Karami and Shankar, [1]). Different axonal volume fractions 40%, 53% and 60% are used to model the unit cell (Karami and Shankar, [1]). For each respective unit cell, maximum and volume average stresses are obtained by applying loads calculated from stretches (1.1, 1.2, 1.3 and 1.4) using experimental data by Velardi et al. [5]. The maximum stresses developed in composite brain tissue will be plotted against respective stretches for each volume fraction and compared with the experimental graphs (stress vs stretch) for *corona radiata.* (Karami and

Shankar, [1]) .The computational results obtained will be compared with the experimental data and an ideal axonal volume fraction will be found out (Karami and Shankar, [1]).

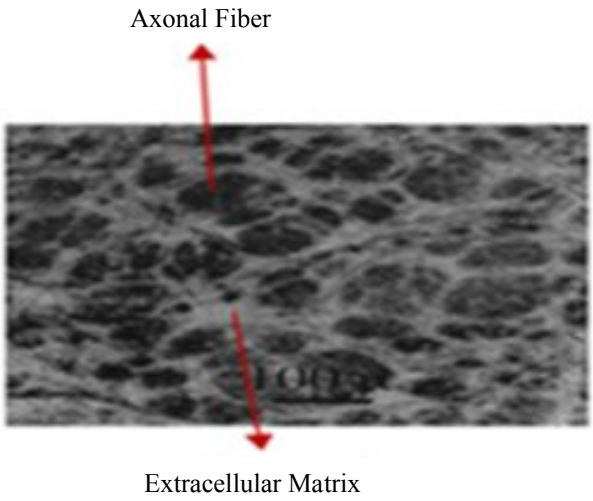

Fig 2. Distribution of axons which are stained dark within the extracellular matrix which are unstained (Arbogast and Margulies, [6]), (Karami and Shankar, [1]).

1.3. Experimental Works

Tensile tests were conducted on porcine brain tissue by Velardi et al. [5] as it has properties identical with brain tissue of humans (Karami and Shankar, [1]). Though there were tests conducted on white matter sheets, corpus collasum and corona radiata but the later is considered here as fibers are assumed to be arranged disorderly which might have bi-directional orientation when compared to the former where there is uniaxial arrangement.

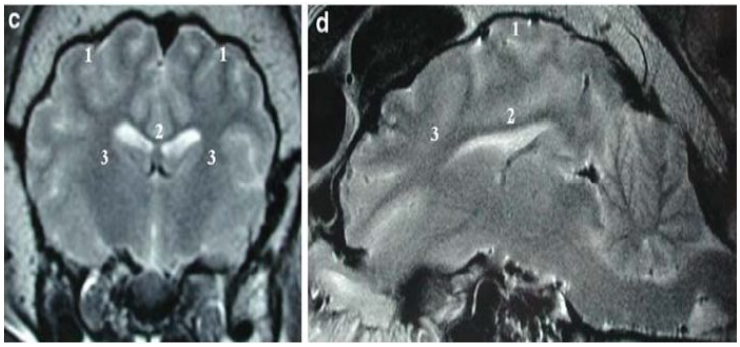

Fig 3. Brain tissue samples of porcine 1= Motor Strip, 2= Corpus Collasum and 3= Corona Radiata (Velardi et. al [5]).

Brain tissue samples of porcine were collected and were cut into several long strips. Velardi et al. [5] tested white matter tissues extracted from *corpus collasum* where axons are distributed longitudinally and *corona radiata* where the fibers are oriented in longitudinal as well as transverse direction (Karami and Shankar, [1]). Total of 24 samples of white matter sheet *corona radiata* for porcine brain tissue were tested by Velardi et.al [5] with (a) 12 fibers oriented in longitudinal pattern and (b) 12 fibers spread in transverse direction. The material property of the tissue were taken to be hyper-elastic and it followed the formulations of Ogden [10] hyper-elastic model. Mass density of white matter was taken to be 1,039 g/cm^3. The cross-sectional areas of the samples were considered as key factors for finding out the loads that were applied on the porcine brain tissue sample and later converted to average stresses. Testing the brain tissue sample strips was not an easy task because of its slippery nature (Karami and Shankar, [1]). It was difficult to place the samples on the testing machine but finally the problem was overcome by adopting some techniques (Karami and Shankar, [1]). "*The samples were dampened by a physiological solution, covered with a tissue paper before placing it into the grips and the grips to hold the samples were tightened manually"*[5], (Karami and Shankar, [1]). The testing machine INSTRON 4301 was used for performing tensile test on the brain tissue strips (Karami and Shankar, [1]). Average stresses were calculated by applying loads obtained from porcine

tissue strips cross section (Karami and Shankar, [1]).CCD camera was placed in front of the testing machine to ensure that the samples did not slip off during the experiment (Karami and Shankar, [1]). With the help of the testing machine load versus displacement graphs were generated and were later used to obtain Stress (S) versus Stretch (λ) plots (Karami and Shankar, [1]). Force divided by initial sample cross-section area taken as average and displacement between samples divided by initial sample length was used to find Stress and Stretch values (Karami and Shankar, [1]). Two plots were obtained for the white matter sheet corona radiata, (i) Stress vs. Stretch plots for axonal fibers oriented in longitudinal direction (Fiber 1) and (ii) Stress vs. Stretch plots for fibers oriented in transverse direction (Fiber 2) (Karami and Shankar, [1]). Velardi et al. [5] considered only the axial loads applied on the porcine brain tissue samples and the experimental plots for *corona radiata* are shown in figures

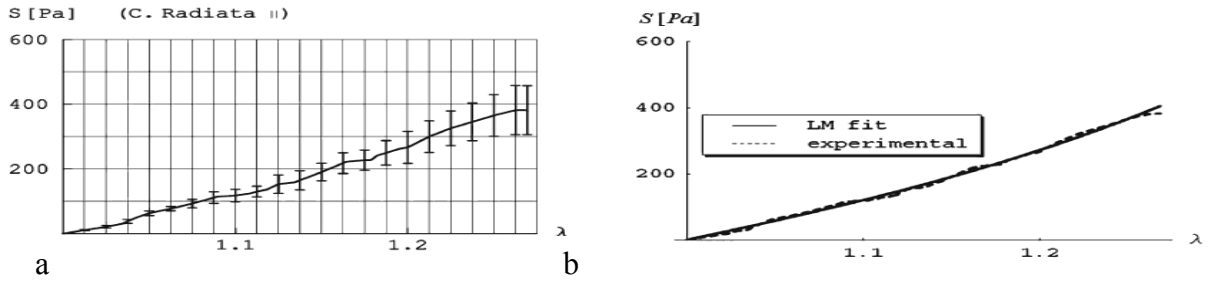

Fig 4. a)Nominal stress (S) against longitudinal stretch (λ) b) Levenberg-Marquardt nonlinear fit method. (Velardi et. al [5]).

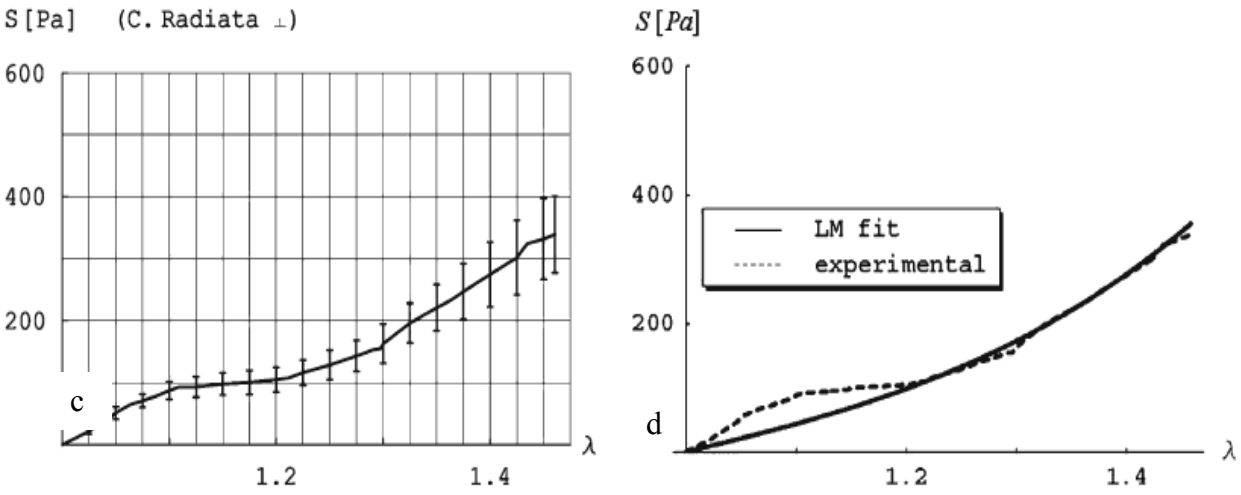

Fig 5. c)Nominal stress (S) against transverse stretch (λ) d) Levenberg-Marquardt nonlinear fit method (Velardi et. al [5]).

1.4. Hyper-Elastic Material Modeling

Hyper-elastic material is a function of strain energy and strain energy as a function of large displacements (Karami and Shankar, [1]). Stress-strain functions define a hyper-elastic material which follows strain energy density equations as suggested by Bhatti [11]. Rubber and brain tissues have material properties similar to a hyper-elastic material as they show non-linear elastic behavior and characteristics of isotropy and incompressibility. Hyper-elastic material exhibits high bulk modulus and large deformations take place here but it has low elastic modulus. Unlike visco-elastic material, hyper-elastic materials undergo large deformations and under large strains they exhibit non-linear elastic behavior up to 500% (Karami and Shankar, [1]). Meaney [12] compared stress vs. stretch plots considering axon microstructure for different hyper-elastic models like (a) Fung formulation, (b) Mooney-Rivlin with that of Ogden model in terms of normal, uniform, empirical frequency distribution and observed that Ogden non-linear model was the most reliable. Stiffness properties for Mooney-Rivlin and neo-Hookean reduced

for given stretch values but the Ogden modeled showed an increase in stiffness for the same set of stretch values as provided by Meaney [12]. Here Ogden [10] hyper-elastic model is taken into account where large deformations take place to analyze the stress-strain relations for materials like brain tissue, rubber etc (Karami and Shankar, [1]).. Ogden [10] hyper-elastic material can undergo a strain till 700% when compared to other models like Mooney Rivilin and Arruda Boyce which have a limit of 200% and 300% strain. (Karami and Shankar, [1]).

Strain energy equation for Ogden [10] hyper-elastic model can be written as (Karami and Shankar, [1]):

$$\text{“}W = 2\mu/\alpha^2 \, (\lambda_1^{\alpha} + \lambda_2^{\alpha} + \lambda_3^{\alpha} - 3) + 2k\mu/\beta^2 \, (I_4^{\beta/2} + 2I_4^{-\beta/4} - 3)$$

$$\lambda_1, \lambda_2, \lambda_3 = 1 \text{ (Karami and Shankar, [1]).}$$

where, $\lambda_1, \lambda_2, \lambda_3$ are taken as principal stretches, I_4 represent the square of material stretch, μ is the infinitesimal shear modulus, k is the stiffness co-efficient and α and β are material parameters [4, 9, 12, 13], (Karami and Shankar, [1]).

1.5. Research Objectives

(a) The extent of axonal stresses developed and deformation occurring in the representative unit cell for the white matter sheet corona radiata will be observed by applying loads, two axial (longitudinal and transverse) and one shear in the form of displacements.

(b) The maximum and average volume normal stresses developed on the overall brain tissue with the average normal stresses in its constituents axon fiber 1, axon fiber 2 compared to extracellular matrix will be found out computationally within the white matter sheet *corona radiata*.

(c) The average volume normal stresses for corona radiata for different axon volume fractions will be compared the experimental data available and an ideal axonal volume fraction for bi-directional distribution of axons will be found out.

In this research work micromechanical principles will be utilized for developing the representative brain tissue models by using the finite element software ABAQUS [2]. The entire modeling of the representative unit cell with that of application of material properties, periodic boundary conditions and load application on the RUC follow a micromechanical tool which will be discussed in detail and the results obtained will be used to characterize the brain tissue.

2. MICROMECHANICAL MODELING OF THE BRAIN TISSUE

2.1. Micromechanical Tissue Characterization Approach

In general the term micromechanics deals with response of the composite type of a material when the geometrical and material parameters of its constituents are known as described by Aboudi [15]. A repeating unit cell (RUC) can be considered a representative volume element which is a point in the continuum space. These repeating unit cells fill up the entire domain and the RUCs behave in an average manner to understand the overall material behavior of the selected region. Homogenous behavior can be achieved by a composite by applying micromechanical principles if it is in a heterogeneous medium. In the field of composite materials, the concept of micromechanics has been very successfully implemented which can characterize the different material parameters like stiffness, strength and fatigue failure. Micromechanical approach can be utilized to analyze the stress-strain developed in the selected material and also give more insight on the deformation occurring in it. The periodic and rigid boundary constraints must be applied on the unit cell in such a way that the surrounding unit cells exhibit the same material response and equal deformation occurs considering the entire domain.

There were several notable works done in the field of micromechanics to characterize the properties of a composite material. The property of a composite material with elastic and non-elastic behavior was studied by Aboudi [15] by utilizing micromechanical principles on the periodic unit cells when there is application of normal loads on the composite. There are several other researchers whose work has been focused on the application of shear loads on the composite such as Needleman and Tvergaard [16]. For the computational analysis in this paper, both normal and shear loads in the form of displacements are applied.

The concept of micromechanics has always been implemented in the field of composites. This theory can further be useful in characterizing the brain tissue models in the area of biomechanics which can be used to study the injury occurring to the axons and extracellular matrix within the white matter of human brain. The deformation of axons within the white matter of the brain tissue will be found out in microscopic level and finally analyzed from macroscopic point of view. By this micromechanical approach, injury caused to the axons can be found out by finding out the stress and strains developed in the individual axons and this might help in for characterizing the brain tissue in macroscopic scale. The white matter in the human brain can be compared to a composite material with axons considered as fibers and extracellular matrix as a matrix. The micromechanical principles can be utilized to comprehend the heterogeneous behavior of the axonal fibers and the base matrix within the white matter. The previously used methods like continuum mechanics and macroscopic analysis of brain tissue is not as efficient as the micromechanical approach as they cannot provide about the accurate development of stress and strains in small scales. Brain stem analysis in order to find out the axonal fiber and base matrix shear modulus was done by Hashin and Rosen [17] by applying micromechanical approach for a viscoelastic material which leads to the development of brain white matter tissue models by Arbogast and Margulies [6]. Further the work was carried on by Meaney [12] to examine the large deformations occurring in the axons surrounded by extracellular matrix for a tissue.

Finite element analysis concepts can be successfully applied to characterize the white matter within the brain tissue by applying micromechanical theories. The axonal fibers with surrounding matrix forming a unit cell can be subjected to various loading conditions by utilizing different micromechanical principles to understand the injury caused to the tissue at a micro

level. The method for modeling and applying loads to the unit cell with axons and base matrix has been developed successfully with the help of micromechanics tool but finding out the material properties of the constituents of the white matter within the brain tissue has always been a difficult task. The micromechanical tool is designed in such a way that it can be used for modeling of axonal fibers oriented in a uniaxial direction as well as bi-directionally. Brain stem is an area within which is located at the posterior portion and is believed to have a uniaxial orientation of axons similar to the white matter sheet *corpus collasum* where the fibers stretch longitudinally. Arbogast and Margulies [6] followed the models proposed by Hashin [17, 18] to examine the properties of the axons and extracellular matrix within the brain stem with fibers oriented uniaxially and reported viscoelastic property for the axonal fibers. Furthermore Ning at al[] also developed same structural models for axons spread on the base matrix oriented in a uniaxial within the brain stem.

The axonal fibers with unidirectional orientation have always been an area for research interest but less work is done in the field of axons distributed bi-axially. There has been some work done by researchers Xia et al. [20], Chen et al. [21] in the field of composites with the fibers oriented in a bidirectional manner. *Corona radiata* is a white matter sheet like *corpus collasum* where axons are said to be oriented in longitudinal direction as well as transverse direction as suggested by Velardi et al. [5]. There were experiments conducted on this white matter tissue by taking samples of porcine brain tissue but computational models are yet to be developed by considering cross-fiber orientation and further examining the stresses, deformations developed on the brain tissue and its constituents by application of loads in the form of displacements by utilizing the concepts of micromechanics.

Finite element software- ABAQUS [2] is used for the characterizing the brain tissue in terms of micromechanical principles. In this paper unit cells which form the representative volume element with known material properties of axons and extracellular matrix will be modeled (Karami and Shankar, [1]). Initially the geometry of the unit cell will be created with axons having cross-fiber orientation within the extracellular matrix. Material data required for the axons and extracellular matrix in developing a 3D model of the unit cell will be input and then with meshing of the cell will be done with precision. After assigning the material property and meshing the geometry, a 'Static General' and assembly of the model should be created for the analysis of the unit cell and further generating input files. After obtaining the input files, periodic boundary constraints will be applied for the micromechanical characterization of the repetitive volume element. The meshing of the 3D unit cell must take place in such a way that the opposite faces of the unit cell deform equally. The mesh developed by ABAQUS software needs further refinement to achieve the goal of exact meshing on opposite faces. A code for implementing periodic boundary conditions is developed by FORTRAN programming by Garnich and Karami [22], Karami and Garnich [23] and Naik et al. [24]. This code along with the other files containing the data for geometry and meshing of the unit cell will be compiled together to replace the input files generated initially with the output file with the periodic boundary codes implemented successfully. This output file which is now taken as the new input file can finally be imported back into the ABAQUS software to finally obtain the model with exact meshing on opposite faces of the cell. Now, loads can be applied one at a time on the different faces of the unit cell to examine the stress contours developed. After application of each load again an input file will be created where a small code is attached to find out the outputs of the data in terms of stress, strain values developed in the unit cell as well as its constituents. This

input file generated after the application of load along with the small FORTRAN code attached will finally create “fil files”, which contains the information for the developed stress, strain values. To interpret these values, a volume average program developed in FORTRAN is used and ABAQUS subroutine is used read the “fil files” and the data from these files determine the overall property of the representative volume element.

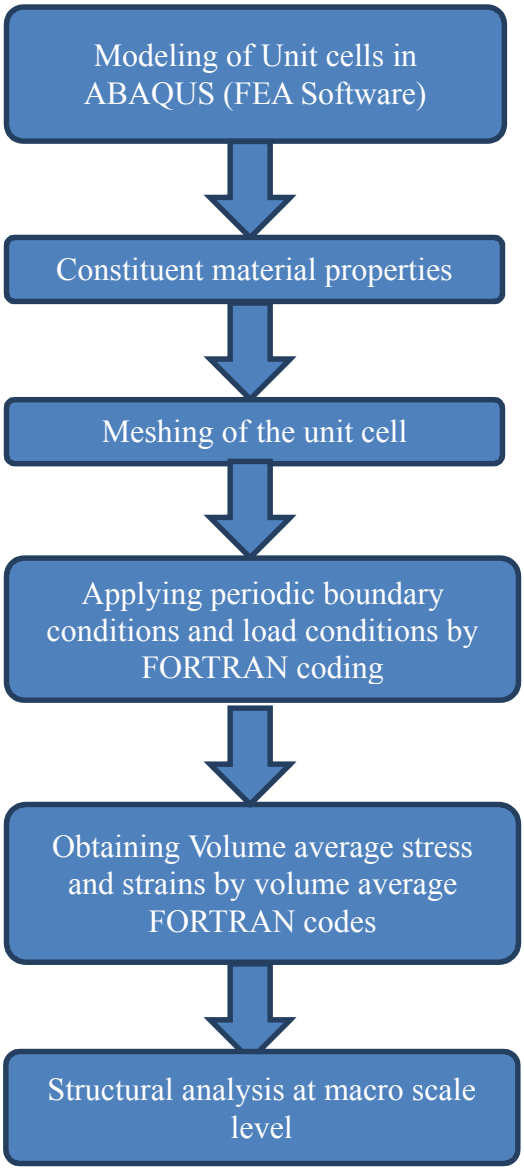

Fig 6. Flow Diagram. Unit cell modeling and structural analysis steps.

2.2. Unit Cell Modeling Procedure

The important parameters for designing a repetitive unit cell are the geometrical specifications and material properties of the individual constituents i.e. axons and extracellular matrix (Karami and Shankar, [1]). The unit cell will represent a three dimensional brain tissue model and when expanded will cover white matter regions of *corona radiata* (Karami and Shankar, [1]). There have been models developed before for axonal fibers oriented in a unidirectional pattern within the white matter but here models for axon fibers in both longitudinal as well as transverse direction will be considered. A rectangular 3D box forming a unit cell is modeled with axons in both longitudinal and transverse orientation while the empty area is occupied by the extracellular matrix. . The orientation of axons for a unit cell within the base matrix is taken to be 90°. These repetitive unit cells comprising of axons and matrix fill up the whole domain where deformations take place equally when there is application of load on this unbounded domain. Loads in the form of displacements are applied on the unit cell and the corresponding deformations and stresses are found out using finite element software- ABAQUS [2], (Karami and Shankar, [1]). After application of loads, volume average stresses and strains are obtained

$$\bar{\sigma}_{ij} \text{ (volume average)} = 1/V * \int_v \sigma_{ij}\, dV$$

$$\bar{\epsilon}ij \text{ (volume average)} = 1/V * \int_v \varepsilon_{ij}\, dV$$

where, V is the volume of the RUC, σ_{ij} *and* ε_{ij} *are distributed stress and strains, respectively,* $\bar{\sigma}_{ij}$ *is volume average stress and* $\bar{\epsilon}_{ij}$ *is volume average strain* [24].

For developing the unit cells certain factors must be considered like the shape, radius, volume fraction percentage and also the number of the axonal fibers. Direction of the axons within the extracellular matrix is another important factor for modeling the unit cells as the

orientation of fibers can be either longitudinal in case of unidirectional fibers and both longitudinal and transverse in case of fibers oriented in a bi-directional manner. It is important to determine the length (l), width (w) and height (h) of the unit cell which are the important parameters for modeling it. Previously there were square unit cells developed for modeling the fiber and matrix within a composite material and here the width (w) is considered equal to its height [24]. Hexagonal unit cells were developed by Karami et al. [8] to represent the distribution of axons within the extracellular matrix considering the hyper-elastic material properties obtained by Meaney [12] from his experiments conducted on guinea pig optic nerve. For modeling this part of brain tissue, unidirectional orientation of axons were considered and the height (h) of the unit cell is equal to $\sqrt{3}$ times width (w). The ideal axon volume fraction for unidirectional orientation of axons was found out to be 53% by Arbogast and Margulies [6]. For modeling the unidirectional orientation of axonal fibers for the brain tissue, Karami et al [8] developed computational unit cell models with axonal volume fractions 40%, 53% and 60% and compared the results with experimental data available.

Modeling the unit cells for the white matter sheet *corona radiata* is different from that of the white matter sheets *corpus collasum* because in this region the axons are distributed in longitudinal and transverse directions. In this case for bi-directional crossed fiber orientation of axons, the lengtht of the repetitive unit cell is equal to 2 times its width. As the unit cell is a point in an infinite domain and hence the exact dimensions needed to model the unit cell are not needed. These dimensions are user defined and for the repeating unit cell they are considered to be 20 mm, 20 mm and 40 mm (width, height and length). Different unit cells comprising of bi-directional pattern of axonal fibers within extracellular matrix are modeled here considering

different axonal volume fractions (40%, 53% and 60%) (Karami and Shankar, [1]). Based on these axonal volume fractions and the dimensions provided for the unit cell, the radius of the axons within the extracellular matrix will be determined and modeled in finite element software ABAQUS [2]. The selected axon volume fractions will be utilized to develop the computational models and will be compared with the experimental data provided by Velardi et al. [5] on the porcine brain tissue strips (Karami and Shankar, [1]). After experimental verification, an ideal axon volume fraction will be reported for bi-directional orientation of axons (Karami and Shankar, [1]).

The radius of the axon required for modeling the unit cell can be found out as follows:

For 40% axon volume fraction;

(Volume of axonal fiber/ Volume of the composite tissue) = 40%

Volume of the fiber = 40%* Volume of the composite

Volume of the fiber is equal to $\pi r^2 h$ which is modeled in a form of a cylinder while the volume of composite tissue is (length* width* height) which is solid rectangle. The number of fibers is taken to be 2.

$(2^* \pi r^2 h) = (40\% * l^* w * h)$.

The length, width and height of the unit cell are 40, 20, and 20 respectively.

Hence the radius for 40% axon volume fraction is calculated to be 7.14 mm and similarly for 53% and 60% volume fractions the radii are found out to be 8.22 mm and 8.74 mm.

Considering these dimensions, various unit cells are modeled by considering hyper-elastic material properties for axons and base matrix for *corona radiata*. After modeling, the

unit cells are meshed in such a manner that the opposite sides of the cell deform symmetrically. (Karami and Shankar, [1])

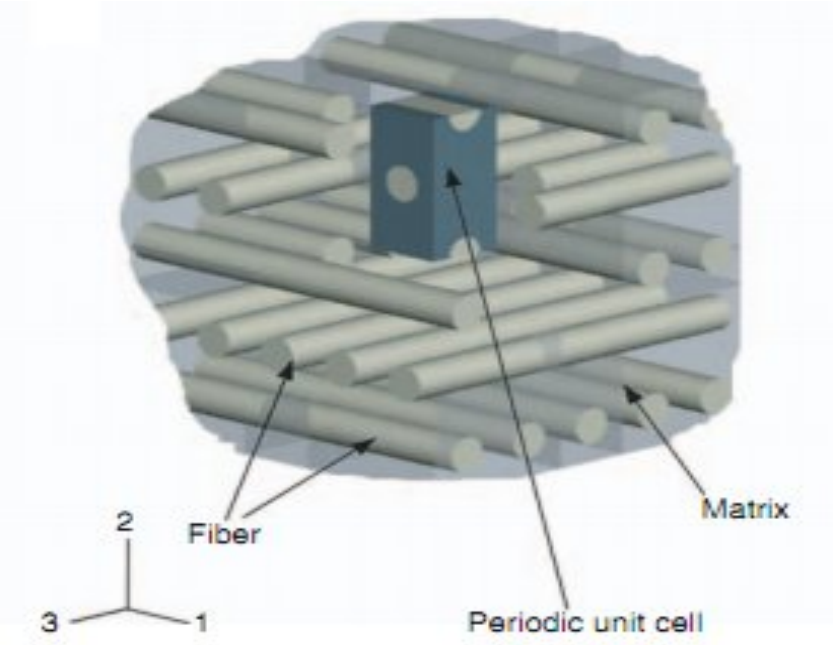

Fig 7. Bidirectional orientation of Axonal Fibers (Naik et al, [24]).

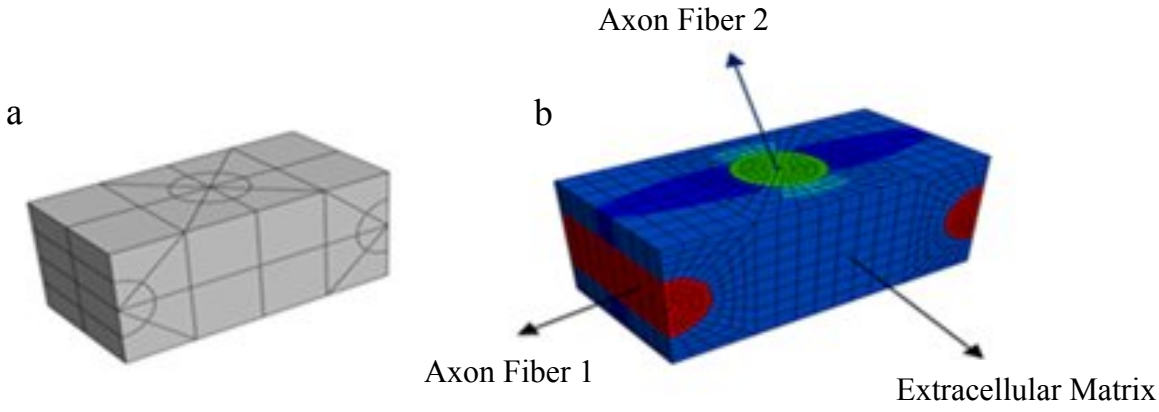

Fig 8. (a) Unit Cell Geometry and (b) Repeating Unit Cell with bi-directional orientation of axons. (Karami and Shankar, [1]).

2.3. Periodic And Rigid Body Constraints

The repeating unit cell which forms a representative volume element is a small part in a selected composite tissue domain which is far from its edge must be implemented with periodic boundary constraints so that it can transfer the response of the material properties developed in the RUC all over the selected continuum domain. The deformation occurring in the selected RUC due to application of load must be transmitted to the neighboring unit cells in an identical way in a particular domain. Finite element methods have been utilized successfully for the implementation of periodic boundary conditions. For crossed fiber orientation of axonal fibers within the extracellular matrix for the white matter tissue *corona radiata,* the angle of the crossing axonal fiber which is taken to be 90º should be constant throughout the selected domain.

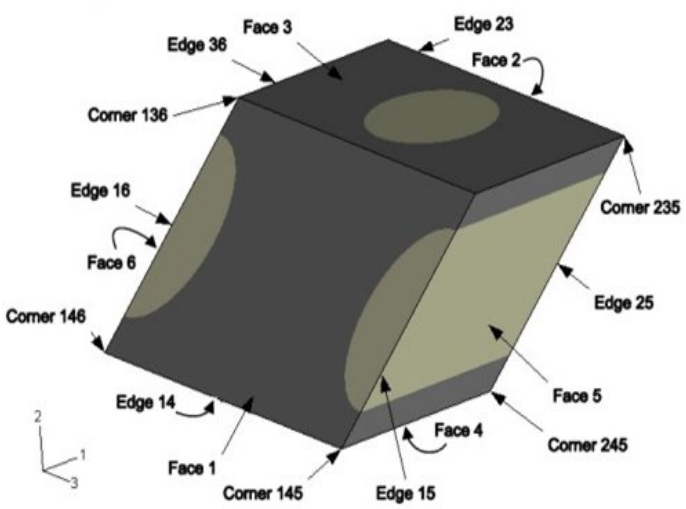

Fig 9. Sample Unit cell with faces, edges and corners. (Abolfathi et al. [7]), (Karami and Shankar, [1]).

Referring to figure 7, the directions 1, 2 and 3 correspond to longitudinal, transverse and transverse normal (Karami and Shankar, [1]). The periodic body constraints must be applied in such a way that the unit cell deforms in a symmetric and identical manner on the reverse sides (Karami and Shankar, [1]). To establish the required symmetry, the number and orientation of nodes on reverse sides of the cell must be equal and similar (Karami and Shankar, [1]). Meshing on the opposite sides of the cell must be identical as it plays an important role here as to achieve the periodic body constraints on the unit cell. Periodic constraints can be applied in an easier way if the faces for each unit cell have a node at its geometric center. Figure 8 consists of 12 edges, 6 faces, 6 face center nodes and 8 corner nodes [7], (Karami and Shankar, [1]). Here faces 2, 4, 6 are opposite to faces 1, 3 and 5 (Karami and Shankar, [1]). The degrees of freedom developed due to displacement of the edges (24, 26, 46…), faces and corners (246…) of one portion of the unit cell must depend on the other half.

The periodic and rigid body constraints applied on a unit cell represented here have been taken from Garnich and Karami [22], Karami and Garnich [23] and Naik et al. [24]. Constraint

equations were developed by the researchers such that reverse faces of the unit cell deform equally. *The displacement taking place in the direction-i is represented as 'U_i' where i= 1, 2, 3 and face center nodes are denoted as C_i where i = 1, 2….6. Similarly N_i and N_j are nodes on opposite faces, N_{ij} represents nodes located on edge which shares the face i, j and N_{ijk} are corner nodes sharing faces i, j, k* [21, 22, 23]. 1, 3 and 5 are the faces which are regarded as the master nodes while the reverse faces 2, 4 and 6 as the slave nodes (Karami and Shankar, [1]).

Face center nodes:

$$\left.\begin{array}{l} U_i^{C_2} + U_i^{C_1} = 0 \\ U_i^{C_3} + U_i^{C_4} = 0 \\ U_i^{C_5} + U_i^{C_6} = 0 \end{array}\right\} \quad \text{……………………………………….. (1)}$$

Node pairs on faces 1and 2:

Considering all surface nodes on faces 1and 2 excepting those on edges sharing faces 2, 4 and 2, 6; corner node sharing faces 2, 4, 6 and center node.

$$U_i^{N_2} + U_i^{C_1} = U_i^{N_1} + U_i^{C_2} \quad \text{………………………………………………. (2)}$$

From equation (1) we obtain

$$U_i^{N_2} - U_i^{N_1} = 2U_i^{C_1} \quad \text{…………………………………………………... (3)}$$

For nodes on edges sharing faces 2, 4 and 2, 6:

$$\left.\begin{array}{l} U_i^{N_{13}} - U_i^{N_{24}} = 2(U_i^{C_1} + U_i^{C_3}) \\ U_i^{N_{15}} - U_i^{N_{26}} = 2(U_i^{C_1} + U_i^{C_5}) \end{array}\right\} \quad \text{………………………………….... (4)}$$

For corner node sharing faces 2, 4 and 6:

$$U_i^{N_{135}} - U_i^{N_{246}} = 2(U_i^{C_1} + U_i^{C_3} + U_i^{C_5}) \quad \text{…………………………………….. (5)}$$

Node pairs on faces 3and 4:

Considering all surface nodes on faces 3and 4 excepting those on edges sharing faces 2, 4 and 4, 6; corner node sharing faces 2, 4, 6 and center node.

$U_i^{N_3} - U_i^{N_4} = 2U_i^{C_3}$ …… (6)

For nodes on edges sharing faces 4, 6:

$U_i^{N_{35}} - U_i^{N_{46}} = 2(U_i^{C_3} + U_i^{C_5})$ …….. (7)

Node pairs on faces 5and 6:

Considering all surface nodes on faces 5and 6 excepting those on edges sharing faces 2, 6 and 4, 6; corner node sharing faces 2, 4, 6 and center node.

$U_i^{N_5} - U_i^{N_6} = 2U_i^{C_5}$ …… (8)

The unit cell must comply with some rigid body constraints in order to avoid unnecessary rotations and translations (Karami and Shankar, [1]). In all directions, the center node of the cell is always fixed (Karami and Shankar, [1]). Translation movement of the unit cell is prevented by keeping the center node of face 1 fixed along direction 1 and to avoid rotational motion, center node on face 2 is fixed along direction 3 (Karami and Shankar, [1]). In order to avoid rigid rotation along directions 2 and 3 of the unit cell, a node is fixed on one of the edges of face 1 (Karami and Shankar, [1]).

2.4. Material Properties Of Brain Tissue

Finding out the material properties of axonal fibers and extracellular matrix in order to characterize the brain tissue has always been a difficult task (Karami and Shankar, [1]). The data available is limited as only a few researchers have conducted experiments on in vivo and in vitro brain tissue (Karami and Shankar, [1]). The process for obtaining the material properties of human brain tissue is very difficult as they are not available in adequate quantity and there are

insufficient dynamic testing methodologies known for finding out the behavior of soft tissues. Porcine brain tissues which can be compared to human tissue were utilized for dynamic testing Snedeker at al. [25] but had some limitations as the strain rates produced were significantly low. The testing techniques adopted by Snedeker et al. [26] for finding out the similarities between porcine and human brain tissues were different. Tests conducted on human brain tissues were almost static while impact loading testing conditions was used to evaluate the properties of porcine brain tissue. Experiments were conducted by Miller and Chinzei [27] on brain tissue samples for swine where compressive loads were applied in uniaxial direction with various strain rate values. Oscillatory testing methodologies were adopted by Arbogast et al. [28] to find out the properties of soft tissue but 20% was the maximum strain achieved by the testing machine and could record a maximum frequency of only 200 Hz. Researchers like Arbogast et al. [28], Miller and Chinzei [27], Arbogast and Margulies [6], Prange and Margulies 2002 [9] and Velardi et al. [5] have produced some substantial work in the field of characterizing the material properties of brain tissues.

Analyzing the material property of the white matter within the brain tissue is very challenging as the axonal fibers exhibit a heterogeneous property embedded within the surrounding extracellular matrix. White matter sheet *corpus collasum* and *brain stem* are parts of the brain where the axonal fibers are distributed in a longitudinal orientation while in the white matter sheet *corona radiata,* the axons are spread in a longitudinal as well as transverse direction.

Arbogast and Marguiles [6] used viscoelastic material properties for axonal fibers and extracellular matrix to characterize the brain tissue within the white matter (Karami and Shankar, [1]). Meaney [12] carried out experiments on guinea-pig optic nerves which is similar to a

human optic nerve and obtained material properties for the axonal fibers (Karami and Shankar, [1]). He used hyper-elastic material to represent his model (Karami and Shankar, [1]). Velardi et al. [5] performed experiments on porcine brain tissue by applying tensile loads and hence acquired the necessary material parameters for the axon using Ogden [10] hyper-elastic model (Karami and Shankar, [1]). Arbogast and Margulies [6] experimentally proposed that axonal fibers are three times stiffer than the extracellular matrix (Karami and Shankar, [1]). For axonal fibers, Velardi et al. [5] provided data for infinitesimal shear modulus μ and two other material parameters α and β whose values remain the same for axon as well as the base matrix (Karami and Shankar, [1]).

Based on these assumptions the material properties of axons and base matrix are considered for the brain white matter *corona radiate* (Karami and Shankar, [1]).

Table 1. Hyperelastic material property for axon and extracellular matrix (Karami and Shankar, [1])

	μ (Pa)	**α**	**β (Pa^{-1})**
Axon	**136.82**	**6.84**	**1.00 E-08**
Extracellular Matrix	**45.6**	**6.84**	**1.00 E-08**

2.5. Loading Scenarios And Conditions

After modeling the unit cells with different axonal volume fractions (40%, 53% and 60%) and assigning the hyper-elastic material properties, the next step required is the application of loads on the unit cell. Previously the researchers have utilized six different loading conditions to analyze the behavior of the unit cell to find out the *anisotropic mechanical properties of brain white matter* [29]. The direction of the axonal fibers was longitudinal and visco-elastic properties obtained by Arbogast and Margulies [6] for characterizing the brain stem was used. For the

analysis of bi-directional orientation of axonal fibers in this thesis, three load cases will be applied on the developed unit cells. Velardi et al [5] during his experiment on white matter sheet *corona radiata,* obtained stretch vs. stress plots for longitudinal as well as transverse directions and hence the first two axial load cases Load case 1 and Load case 2 will be applied to verify the experimental results computationally. The third load case is shear in nature and is applied to study the injury occurring due to development of shear forces in the axons which is responsible for Diffuse Axonal Injury.

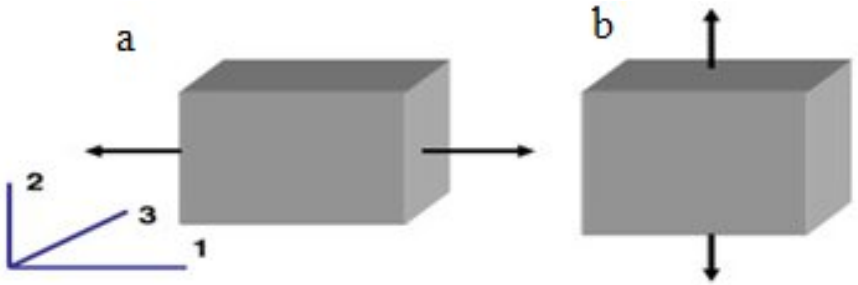

Fig 10. (a) Load case 1 and (b) Load case 2 (Abolfathi et al. [7]), (Karami and Shankar, [1]).

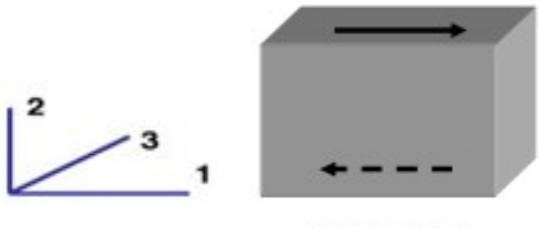

Fig 11. Load case 3 (Abolfathi et al. [7]), (Karami and Shankar, [1]).

In figure 8(a), the applied load 1 is axial and the direction is longitudinal while in 8(b), load 2 is axial and transverse and for figure 9, the applied load 3 is shear (Karami and Shankar,

[1]). The load 1 on the unit cell is tensile and is applied on face 1 center node along direction 1, load 2 is applied on the center node of face 3 along direction 2 and load 3 is applied in direction 1 on the center node of face 3 as can be seen in Fig 7 (Karami and Shankar, [1]).

Loads applied on the periodic unit cell are calculated by considering the displacements resulting due to stretches (λ) as hyper-elastic material is a function of strain energy and strain energy as a function of large displacements (Karami and Shankar, [1]). The stretch (λ) values are taken to be 1.1, 1.2, 1.3 and 1.4 which are taken from the experimental results obtained by Velardi et al. [5] on the strips of porcine brain tissue (Karami and Shankar, [1]).

For each axonal volume fraction (40%, 53% and 60%), displacements were calculated and hence simulations were run for stretches 1.1, 1.2, 1.3 and 1.4 to obtain the axonal deformation and stresses developed in each element which are later utilized to compute the volume average stresses. The overall behavior of the hyper-elastic material can be understood by plotting volume average stresses vs. stretch graphs (Karami and Shankar, [1]).

3. STUDYING THE RESPONSE OF TISSUE UNIT CELLS

3.1. Tissue Unit Cells Under Axial Loading

The unit cells modeled here will be exposed to two types of axial loading (a) Load Case-1 and (b) Load Case-2 where the loads applied in the form of displacements are Longitudinal and Transverse. These two load cases will be applied on the unit cells modeled with different axonal volume fractions 40%, 53% and 60% to obtain computational results and will be compared to stress vs. stretch plots obtained experimentally for white matter sheet *corona radiata* by Velardi et al. [5] to obtain an ideal axon volume fraction for bi-directional orientation of fibers (Karami and Shankar, [1]). The ideal axon volume fraction for uni-directional orientation of axon fibers was obtained by Arbogast and Margulies [6] for the white matter sheet *corpus collasum* which was reported to 53%.

For different volume fractions 40%, 53% and 60%, stress contour plots for the deformations on the composite brain tissue are obtained but plots for only 40% axon volume fraction are displayed here (Karami and Shankar, [1]). For load cases, 1 and 2 stress contour plots are shown in figures (10,11) and (17, 18) calculated from the respective stretches 1.1, 1.2, 1.3 and 1.4, the same values taken by Velardi et al. [5] for conducting his experiments. After plotting the stress contours, the values for maximum normal stresses, average volume normal stress, volume average stresses for axon fiber 1, axon fiber 2 and extracellular matrix of the tissue are obtained for load case 1 and 2 by using volume average subroutine for different volume fractions as shown in tables 2 and 3. Plots for maximum normal stresses developed on the white matter sheet *corona radiata* for the brain tissue, average volume normal stresses in the brain tissue and volume average stresses in its constituents (Karami and Shankar, [1]); axonal fiber 1, axonal fiber 2 and extracellular matrix for each volume fraction are obtained considering

load cases 1 and 2 shown in figures 12, 13, 14, 15, 16 and 19, 20, 21, 22, 23. In case of maximum normal stresses for each volume fraction considered, stress vs. stretch graphs is obtained and volume average stresses in axon fiber 1, axon fiber 2 and extracellular matrix are plotted against the stretch values to understand the overall effect on the brain tissue (Karami and Shankar, [1]). After plotting the results, stresses developed on the tissue are compared for Load case 1 and Load case 2.

Calculation of displacements in the form of loads: The material used for the constituents axon and extracellular matrix is hyper-elastic. Hyper-elastic material is a function of strain energy and strain energy as a function of large displacements (Karami and Shankar, [1]). *Velardi et al. [5] calculated loads in the form of displacements from the tissue sample cross-section areas which were finally converted into average stresses.* The stretch values taken from the experimental data are 1.1, 1.2, 1.3 and 1.4. Load case – 1 is applied on the center node of face 6 along direction 1 of the unit cell and Load case – 2 is applied on the center node of face 3 along direction 2 of the unit cell as can be seen in Fig. 7 (Karami and Shankar, [1]).

$$\text{Stretch } (\lambda) = (\text{Final Length after deformation})/\text{Initial Length}$$

$$= (L+\Delta L)/L$$

where L = Initial Length and ΔL = Displacement occurring due to deformation.

For load case 1, direction 1 which is the width of the unit cell taken as the initial length where the displacement is applied = 20 mm.

For load case 2, direction 2 which is the height of the unit cell taken as the initial length where the displacement is applied = 20 mm.

The calculated displacements for the respective stretches 1.1, 1.2, 1.3 and 1.4 are 2 mm, 4 mm, 6 mm and 8 mm.

3.1.1. Load Case 1 (Axial Loading- Longitudinal) (Karami and Shankar, [1])

In figures 10 and 11, tensile loads are applied on the central node of face 6 (Fig. 7) along direction 1.

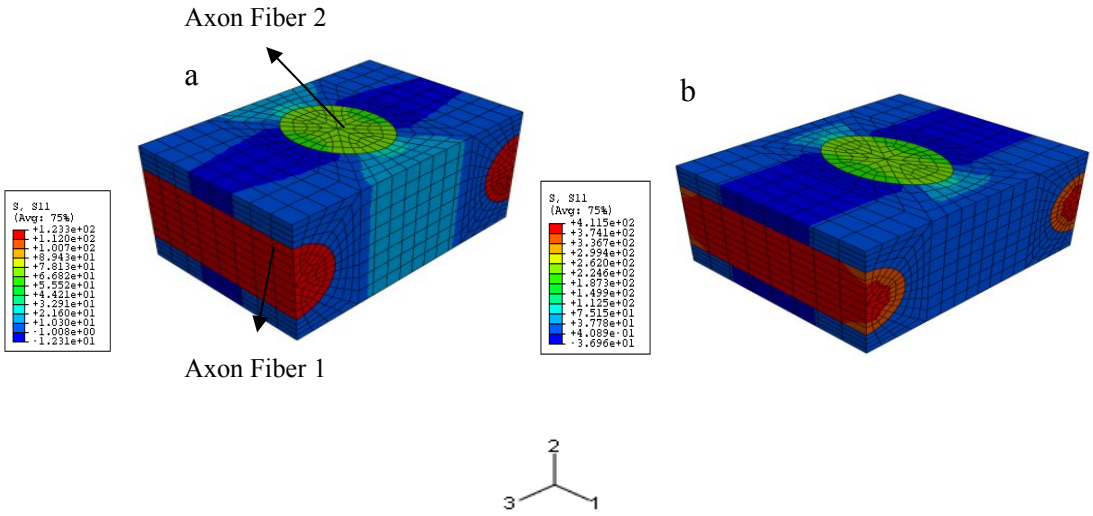

Fig 12. Contour of normal stress plots for load case 1 with an axonal fiber volume fraction of 40% (a) Stretch 1.1 and (b) Stretch 1.2 (Karami and Shankar, [1]).

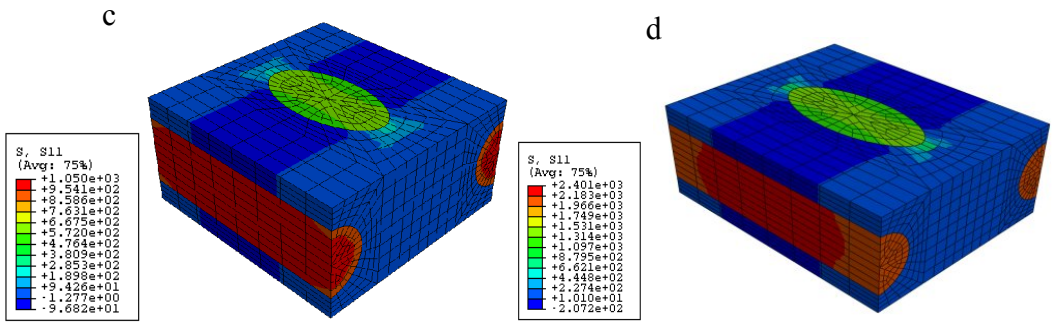

Fig 13. Contour of normal stress plots for load case 1 with an axonal fiber volume fraction of 40% (c) Stretch 1.3 and (d) Stretch 1.4 (Karami and Shankar, [1]).

Table 2. Stress values obtained for Load Case 1 (Karami and Shankar, [1])

Axon Volume Fraction %	Stretch	Maximum normal stress of the tissue (Pa)	The average volume normal stress of the tissue (Pa)	Average normal stress of axon fiber 1 (Pa)	Average normal stress of axon fiber 2 (Pa)	Average normal stress of ECM (Pa)
40%	1.1	60	18.5	118.3	68.7	45.7
	1.2	198	53.7	388.5	228.9	150.6
	1.3	505	104.51	991.8	580.4	385.7
	1.4	1140	182.4	2236.5	1340.9	861.1
53%	1.1	64.2	27.01	118.3	72.7	47
	1.2	212	66.5	388.9	239.96	155.4
	1.3	540	114.8	992.7	612.7	396.9
	1.4	1220	202.5	2235	1378.7	892.4
60%	1.1	75.5	32.1	118.4	83.6	50.2
	1.2	249	73.9	389.4	257.2	165.9
	1.3	634	131	994.6	698.6	424.9
	1.4	1430	285.1	2243.8	1588	946.8

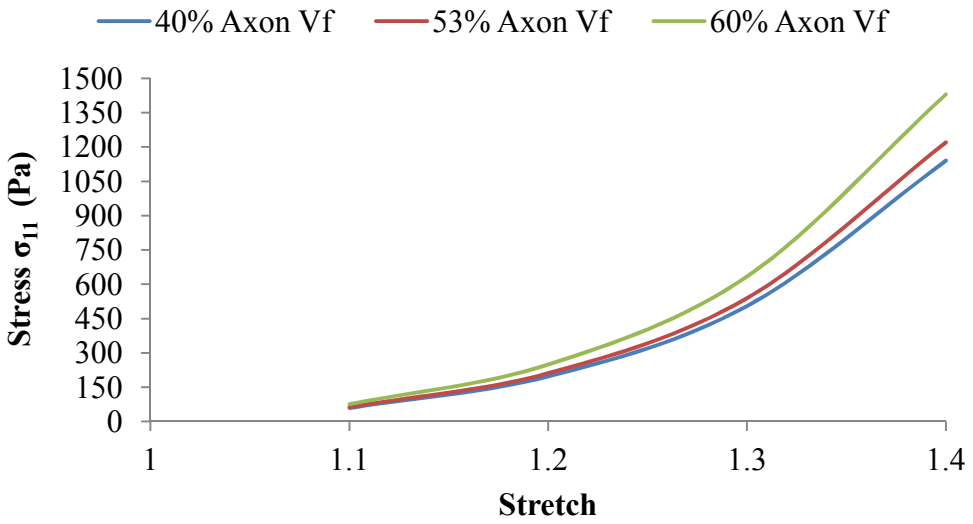

Fig 14. Load Case 1. Maximum Normal Stresses developed in *corona radiata* for 40%, 53% and 60% axon volume fractions with displacement in the form of load applied in direction 1, 1 (Fig 7) (Karami and Shankar, [1]).

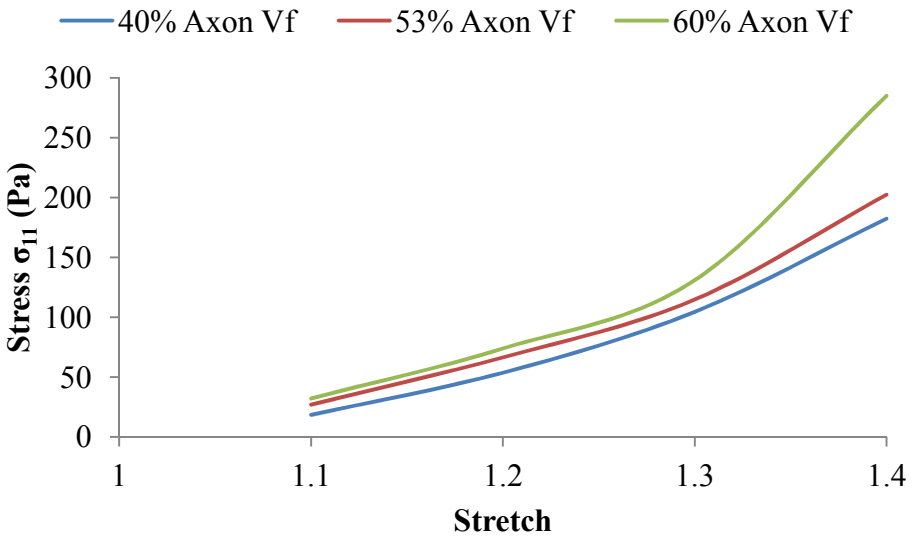

Fig 15. Load Case 1. Average Volume Normal Stresses developed in *corona radiata* for 40%, 53% and 60% axon volume fractions with displacement in the form of load applied in direction 1, 1 (Fig 7) (Karami and Shankar, [1]).

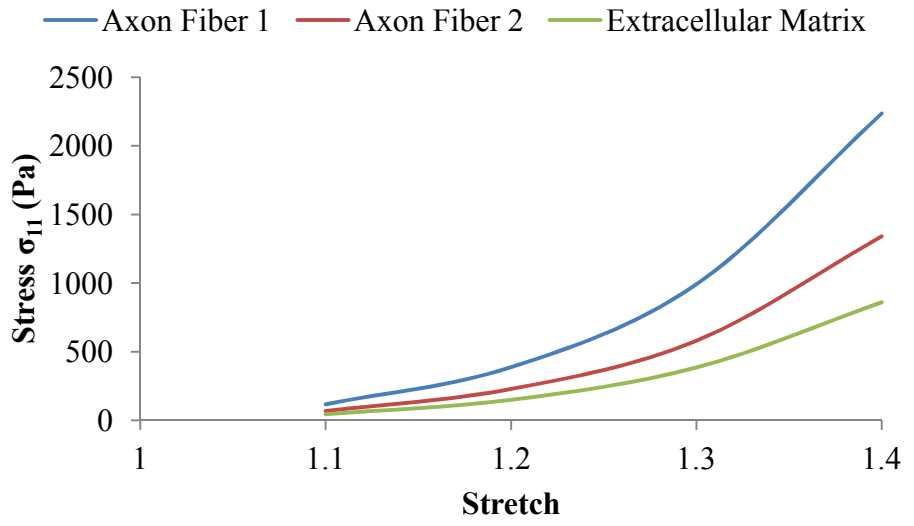

Fig 16. Load Case 1. Average normal stress developed in Axon Fiber 1, 2 and Extracellular Matrix for 40% axon volume fraction with displacement in the form of load applied in direction 1, 1 (Fig 7) (Karami and Shankar, [1]).

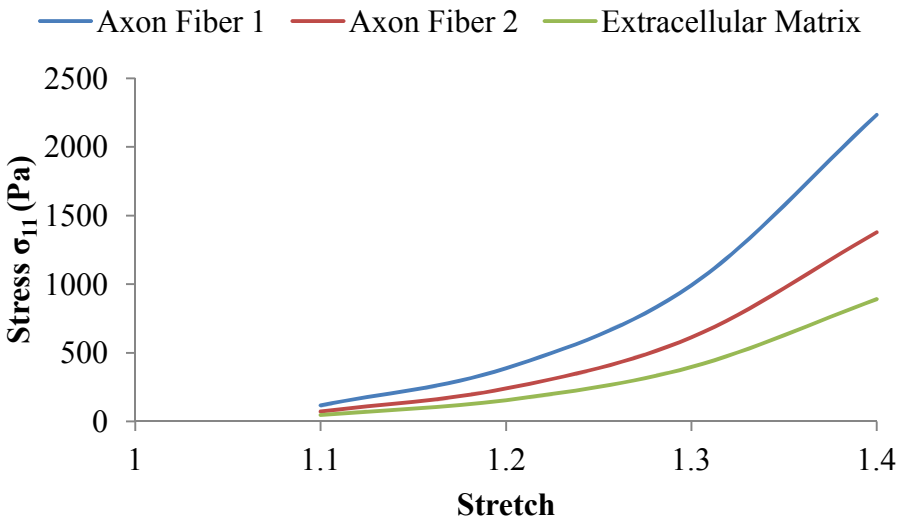

Fig 17. Load Case 1. Average normal stress developed in Axon Fiber 1, 2 and Extracellular Matrix for 53% axon volume fraction with displacement in the form of load applied in direction 1, 1 (Fig 7) (Karami and Shankar, [1]).

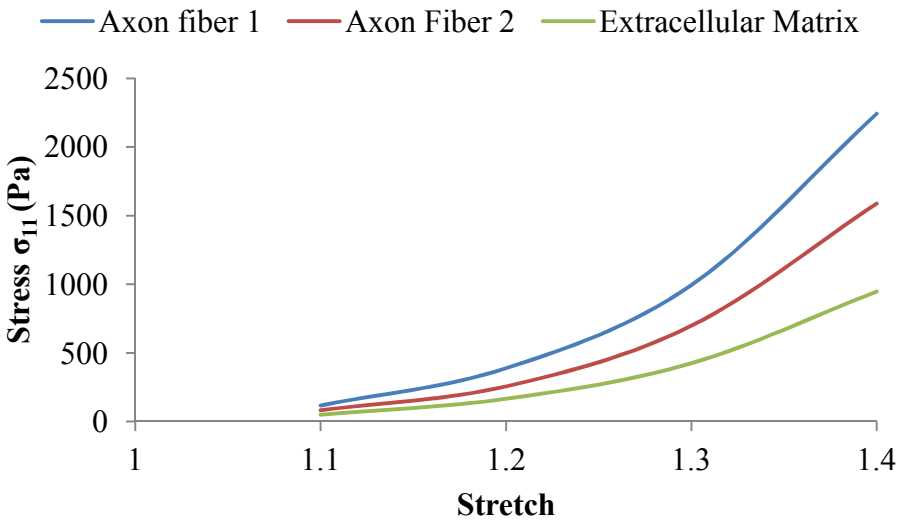

Fig 18. Load Case 1. Average normal stress developed in Axon Fiber 1, 2 and Extracellular Matrix for 60% axon volume fraction with displacement in the form of load applied in direction 1, 1 (Fig 7) (Karami and Shankar, [1]).

3.1.2. Load Case 2 (Axial Loading-Transverse) (Karami and Shankar, [1])

In figures 17 and 18, tensile loads are applied on the central node of face 3 (Fig. 7) along direction 2.

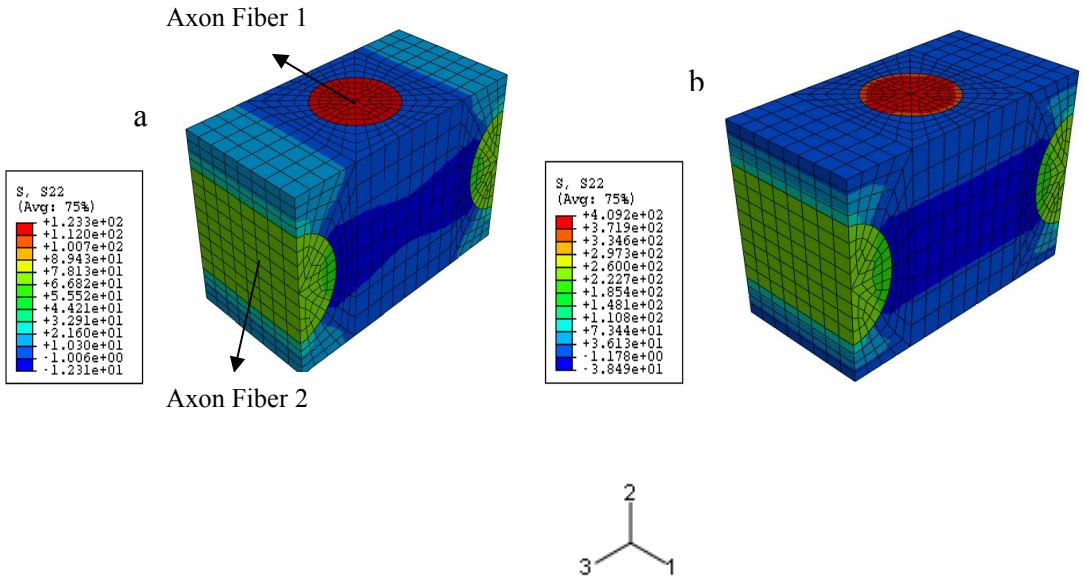

Fig 19. Contour stress plots for load case 2 with an axon volume fraction of 40% (a) Stretch 1.1 and (b) Stretch 1.2 (Karami and Shankar, [1]).

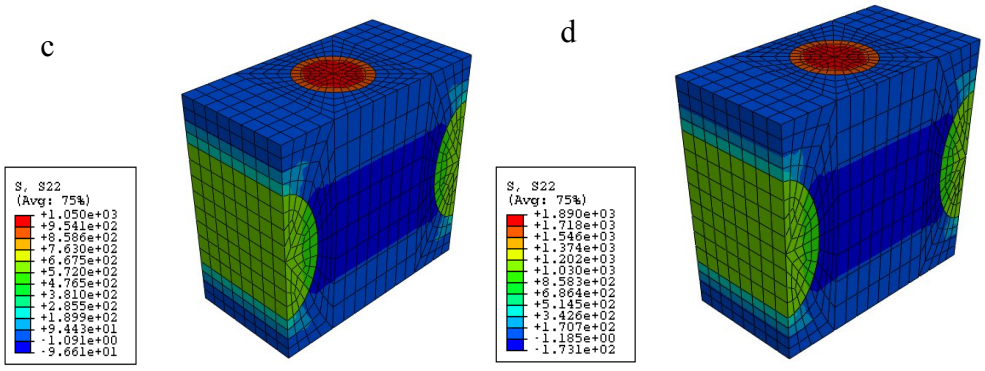

Fig 20. Contour stress plots for load case 2 with an axon volume fraction of 40% (c) Stretch 1.3 and (d) Stretch 1.4 (Karami and Shankar, [1]).

Table 3. Stress values obtained for Load Case 2 (Karami and Shankar, [1])

Axon Volume Fraction %	Stretch	Maximum normal stress of the tissue (Pa)	The average volume normal stress of the tissue (Pa)	Average normal stress of axon fiber 1 (Pa)	Average normal stress of axon fiber 2 (Pa)	Average normal stress of ECM (Pa)
40%	1.1	59.9	23.8	68.7	118.3	45.7
	1.2	197	53.8	227.1	388.3	150.7
	1.3	504	103.7	580.2	991.8	384.7
	1.4	906	162.5	1042.8	1783.5	691.2
53%	1.1	64.1	26.2	72.7	118.3	46.9
	1.2	211	58.5	239.9	388.6	154.9
	1.3	540	121.9	612.9	992.7	395.6
	1.4	1210	186.5	1379	2235	889.3
60%	1.1	75.4	29.7	83.7	118.5	50.1
	1.2	248	70.1	275.2	389.5	165.3
	1.3	634	145.7	703.9	995.7	420.7
	1.4	1430	276.4	1589.7	2244	942.3

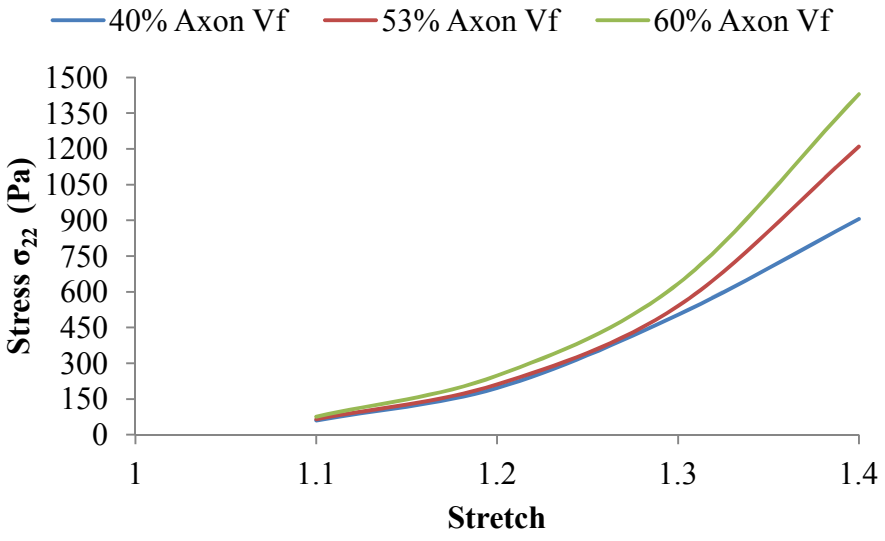

Fig 21. Load Case 2. Maximum Normal Stresses in *corona radiata* for 40%, 53% and 60% axon volume fractions with displacement in the form of load applied in direction 2,2 (Fig 7) (Karami and Shankar, [1]).

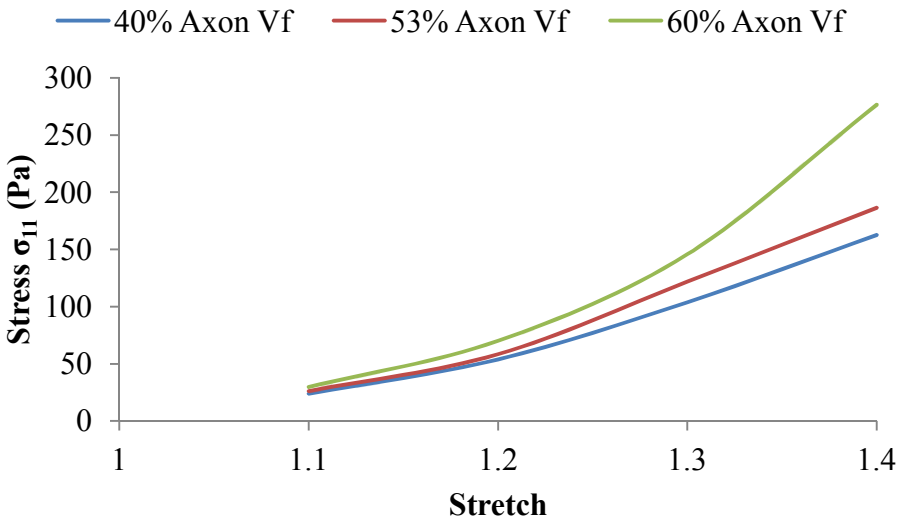

Fig 22. Load Case 2. Average Volume Normal Stresses in *corona 36adiate* for 40%, 53% and 60% axon volume fractions with displacement in the form of load applied in direction 2, 2 (Fig 7) (Karami and Shankar, [1]).

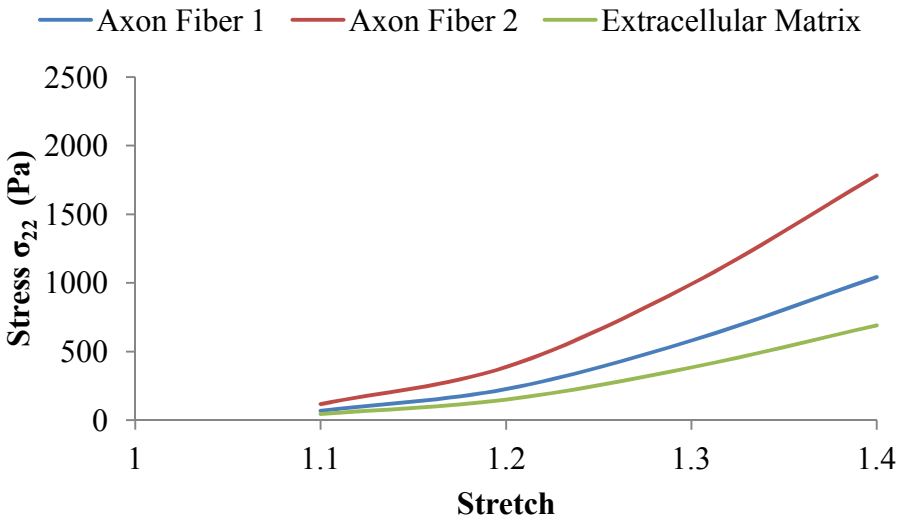

Fig 23. Load Case 2. Average normal stress in Axon Fiber 1, 2 and Extracellular Matrix for 40% axon volume fraction with displacement in the form of load applied indirection 2, 2 (Fig 7) (Karami and Shankar, [1]).

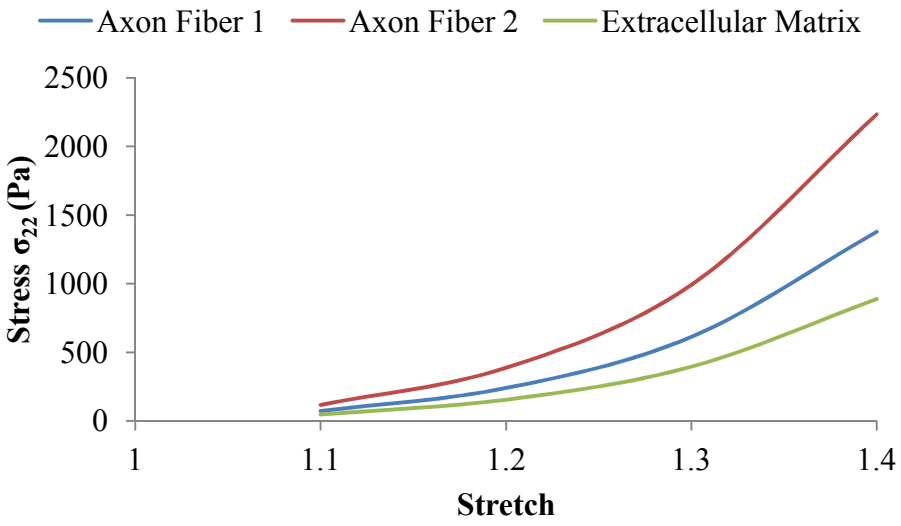

Fig 24. Load Case 2. Average normal stress in Axon Fiber 1, 2 and Extracellular Matrix for 53% axon volume fraction with displacement in the form of load applied in direction 2, 2 (Fig 7). (Karami and Shankar, [1]).

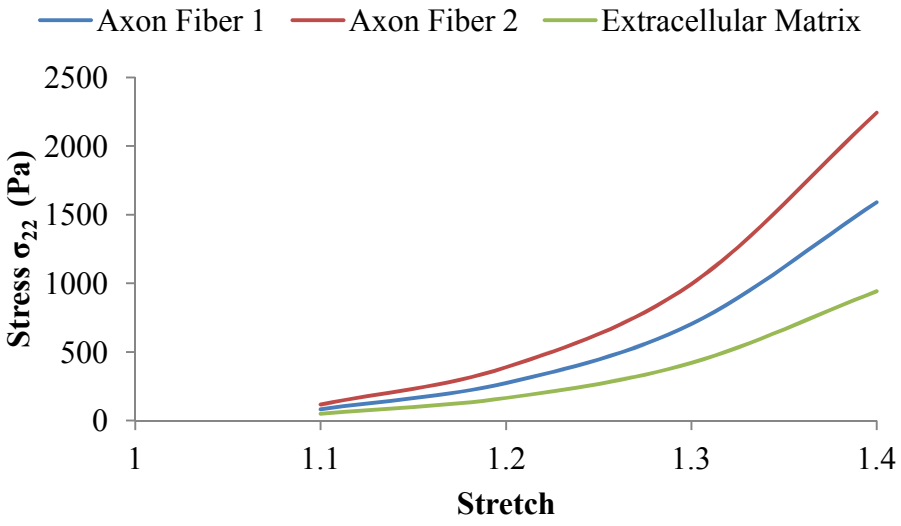

Fig 25. Load Case 2. Average normal stress in Axon Fiber 1, 2 and Extracellular Matrix for 60% axon volume fraction with displacement in the form of load applied in direction 2, 2 (Fig 7) (Karami and Shankar, [1]).

3.2. Discussions For Load Case 1 And Load Case 2

Axonal injury takes place in case of mishaps like explosions, small and severe accidents, falling from heights causing DAI where axons are elongated and deformed. This deformation and elongation of the axonal fibers can be seen in figures 10, 11 and 17, 18 for load cases 1 and 2 (Karami and Shankar, [1]). The stresses developed on white matter sheet *corona radiata* and on axons as well as extra-cellular matrix are reported in Table 2, 3 (Karami and Shankar, [1]). The plot in figures 12 and 19 tells about the maximum stress developed in the brain tissue under load conditions 1 and 2 (Karami and Shankar, [1]). Unit cells with different volume fractions (V_f) 40%, 53% and 60% were modeled and loads were applied on these unit cells in the form of displacements which were in longitudinal direction (Load Case 1) and the other in transverse direction (Load Case 2) (Karami and Shankar, [1]). In case of load case 1, the stiffer axons were greater in axons with higher volume fractions because the stresses developed here were larger than the stresses developed in axons with low volume fraction (Karami and Shankar, [1]). It was found that average volume normal stress of the tissue for an axon V_f of 60% is 2.7 times greater than 40% V_f and 1.4 times greater than 53% V_f for a given stretch of 40% (Karami and Shankar, [1]). When considering load case 2, the average volume normal stress of the tissue for an axon V_f of 60% is 1.7 times greater than 40% V_f and 1.5 times greater than 53% V_f for a given stretch of 40% (Karami and Shankar, [1]). Axons with higher volume fractions exhibited higher stress values in case overall tissue as well as axon fiber 1, 2 and the extracellular matrix (Karami and Shankar, [1]).

For both load case 1 and load case 2, volume average stresses developed in axon fiber 1, 2 and extracellular matrix can be compared (Karami and Shankar, [1]). In case of load case 1 for 40% axon V_f, stress in axon fiber 1 is almost 2.5 times greater than the extracellular matrix while

for 53% and 60%, the stress developed is 2.5 and 2.35 times greater than the extracellular matrix (Karami and Shankar, [1]). Here axon fiber 2 for 40% V_f is about 1.5 times and for 53% and 60%, V_f is 1.5 and 1.67 times larger than the base matrix (Karami and Shankar, [1]). In case of load 2 for 40% axonal V_f, stress in axon fiber 1 is 1.5 times more than the extracellular matrix while for 53% and 60%, the stress developed is 1.5 times and 1.67 times greater than the extracellular matrix (Karami and Shankar, [1]). Axon fiber 2 for 40% V_f is about 2.5 times and for 53% and 60%, V_f is 2.5 and 2.35 times greater than the base matrix (Karami and Shankar, [1]). Considering the stresses developed in Axon Fiber 1 which is the longitudinal direction, load case 2 is more evenly distributed than load case 1 (Karami and Shankar, [1]). But for Axon Fiber 2 which is the transverse direction, stresses in load case 1 are more evenly distributed than load case 2 (Karami and Shankar, [1]).

3.3. Tissue Unit Cells Under Shear Loading

Diffuse Axonal Injury occurs due to development of shear forces in the axons and hence unit cells are modeled to study the stresses developed on the brain tissue as well as its constituents; axons and extracellular matrix due to application of of shear displacements. The experimental data available for the brain tissue under shear loads is not sufficient and hence the model developed computationally cannot be compared to the experimental model.

Load case – 3 which is the shear load is applied on the center node of face 3 along direction 1 as seen in figure 8 (Karami and Shankar, [1]). The displacements 2 mm, 4 mm, 6 mm and 8 mm are used to find out the angles(α) at which the shear displacement occurs in the direction of longitudinal axis of axon fiber 1 which are calculated to be 11.3º, 21.8º, 30.9º and 38.7º . The stress contour plots for the deformations on the composite brain tissue under shear

loading are obtained but plots for only 40% axon volume fraction are displayed as seen in figures 24 and 25. Values for maximum normal stresses, average volume normal stress, volume average stresses for axon fiber 1, axon fiber 2 and extracellular matrix developed in the brain tissue are obtained for load case 3 under shearing effect by using volume average subroutine for different volume fractions as shown in Table 4. Plots for maximum normal stresses developed on the white matter sheet *corona radiata* for the brain tissue and volume average stresses in its constituents; axonal fiber 1, axonal fiber 2 and extracellular matrix for each volume fraction are obtained considering load case 3 shown in figures 26, 27, 28 and 29 (Karami and Shankar, [1]).

Load case 3 (Shear Loading)

Shear load is applied on the center node of face 3 along direction 1 (Fig 7) (Karami and Shankar, [1]).

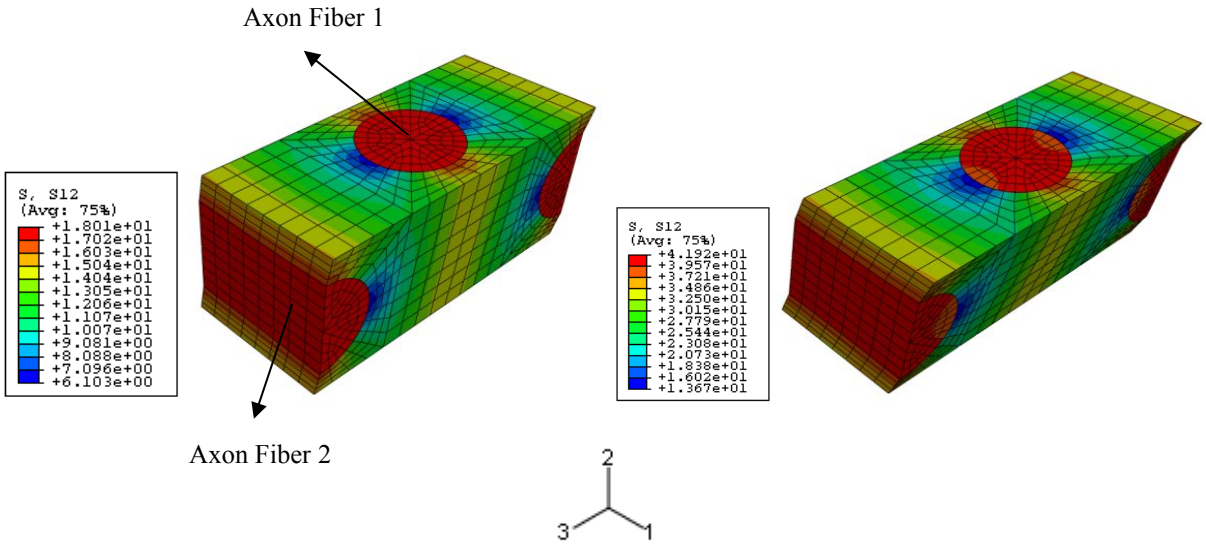

Fig 26. Contour shear stress plots for load case 3 with an axon volume fraction of 40%. Shear stress developed at an angle of (a) 11.3° for a displacement of 2mm and (b) 21.8° for a displacement of 4mm (Karami and Shankar, [1]).

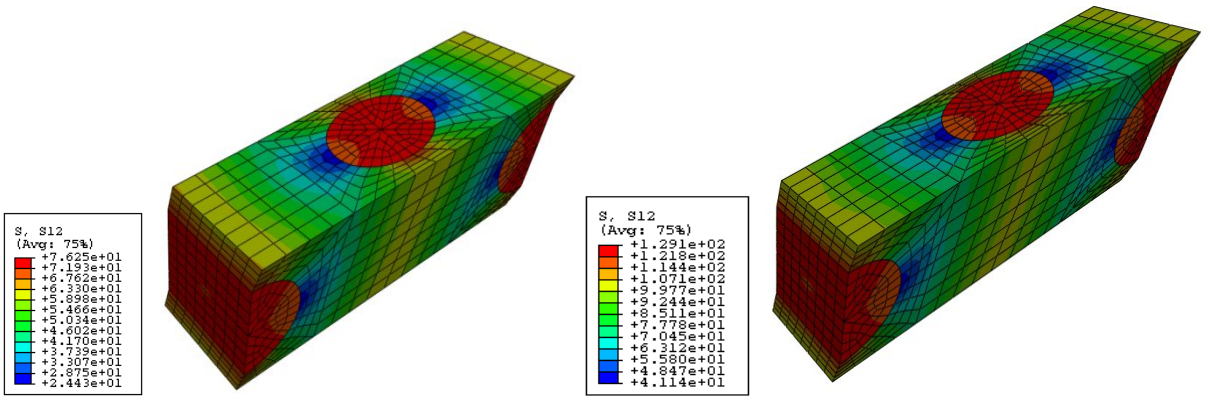

Fig 27. Contour shear stress plots for load case 3 with an axon volume fraction of 40%. Shear stress developed at an angle of (a) 30.9° for a displacement of 6mm and (b) 38.7° for a displacement of 8mm (Karami and Shankar, [1]).

Table 4. Stress values obtained for Load Case 3 (Karami and Shankar, [1])

Axon Volume Fraction %	Required Displacement (mm)	Angle(α) at which shear displacement occurs in the direction of longitudinal axis of axon fiber 1	Maximum normal shear stress of the tissue (Pa)	The average volume normal shear stress of the tissue (Pa)	Average normal shear stress of axon fiber 1 (Pa)	Average normal shear stress of axon fiber 2 (Pa)	Average normal shear stress of ECM (Pa)
40%	2	11.3º	.763	.388	17.3	19.7	10.42
	4	21.8°	.936	.685	39.9	45.6	24
	6	30.9°	3.2	1.52	72.4	82.8	43.6
	8	38.7°	24.7	3.71	123.1	140.8	74.1
53%	2	11.3º	2.33	.479	18	20.52	10.8
	4	21.8°	2.56	.779	41.4	47.3	24.9
	6	30.9°	9.21	1.63	75.1	86.1	45.3
	8	38.7°	34.1	4.62	127.5	145.9	76.8
60%	2	11.3º	3.9	1.75	19.9	22.2	11.1
	4	21.8°	11.3	4.06	45.9	50.8	25.5
	6	30.9°	26.9	7.61	82.7	91.6	45.9
	8	38.7°	61.6	12.5	140.6	156.4	78.1

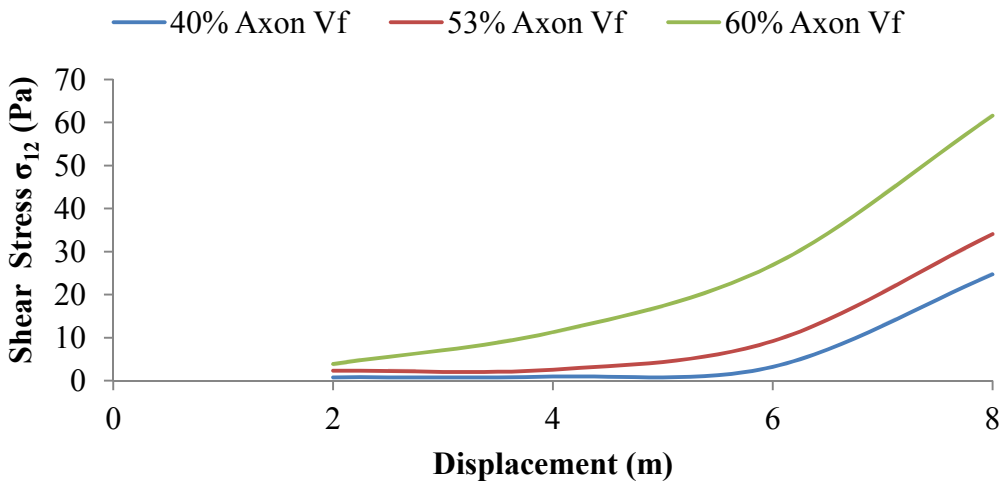

Fig 28. Load case 3. Maximum Normal shear stresses in *corona radiata* for 40%, 53% and 60% axon volume fractions with displacements applied in direction 1, 2 (Fig 7)
(Karami and Shankar, [1]).

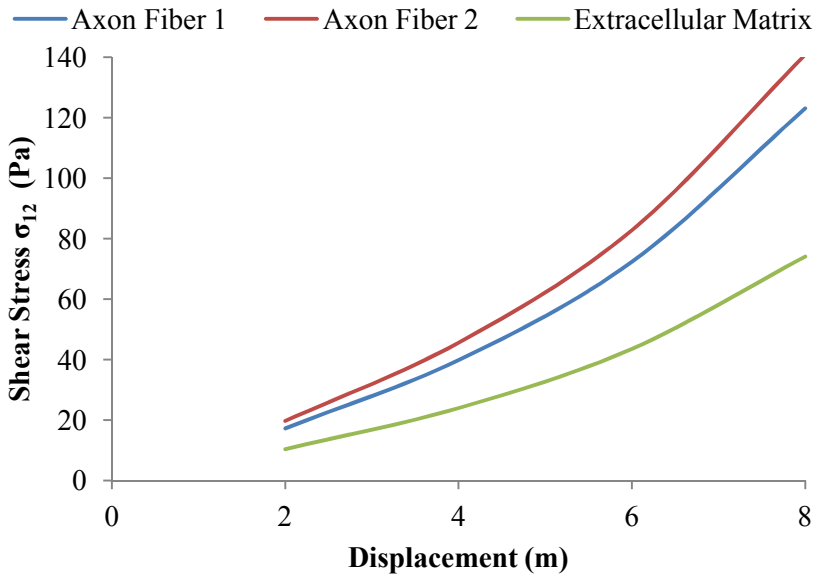

Fig 29. Load case 3. Average normal shear stress in axon fiber 1, 2 and extracellular matrix for 40 % axonal volume fraction fractions with displacements applied in direction 1, 2 (Fig 7) (Karami and Shankar, [1]).

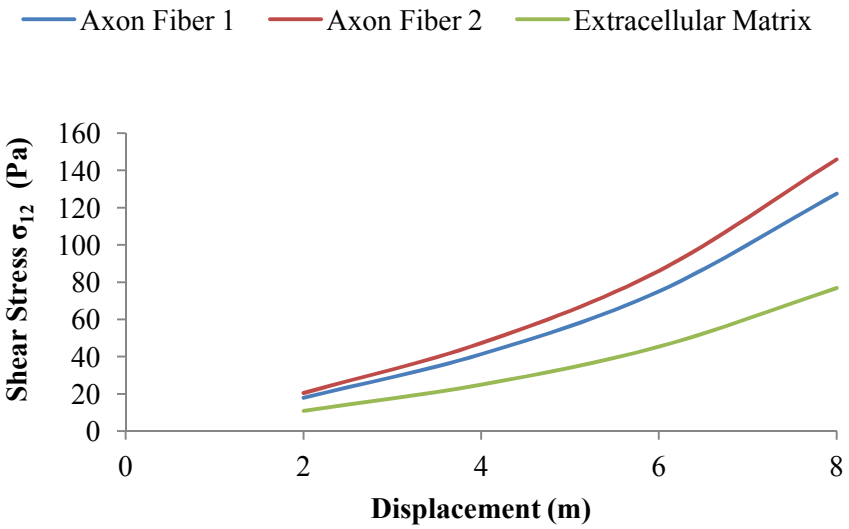

Fig 30. Load case 3. Average normal shear stress in axon fiber 1, 2 and extracellular matrix for 53 % axonal volume fraction fractions with displacements applied in direction 1, 2 (Fig 7) (Karami and Shankar, [1]).

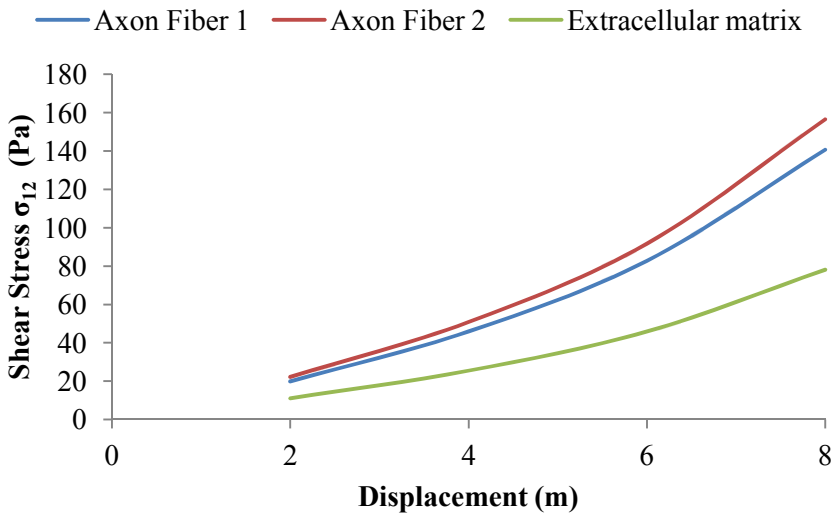

Fig 31. Load case 3. Average normal shear stress in axon fiber 1, 2 and extracellular matrix for 60 % axonal volume fraction fractions with displacements applied in direction 1, 2 (Fig 7) (Karami and Shankar, [1]).

Experiments were conducted on brain tissue by Velardi et al. [5] for loads in longitudinal and transverse direction but shear load must also be considered (Karami and Shankar, [1]). The prime reason for DAI is shear forces developing on the axons and hence causing damage to it (Karami and Shankar, [1]). Here computational results for development of shear stress are found out by applying displacements in the form of loads at different angles (Karami and Shankar, [1]). Considering longitudinal and transverse directions for load case 1 and load case 2, the computational data obtained for maximum normal stress developed in the tissue is almost the same but different when compared to the maximum shear stress developed in the tissue (Karami and Shankar, [1]). This indicates that brain tissue under shear loading is affected more when compared to axial loads. In case of load case 3 for 40% axon V_f, stress in axon fiber 1 is almost 1.66 times greater than the extracellular matrix while for 53% and 60%, the stress developed is

1.66 and 1.8 times greater than the extracellular matrix (Karami and Shankar, [1]). Here axon fiber 2 for 40% V_f is about 1.9 times and for 53% and 60%, V_f is 1.9 and 2 times larger than the base matrix (Karami and Shankar, [1]). The values obtained for average normal shear stress for axon fiber 1 and axon fiber 2 for load case considering different axon volume fractions are almost same thus indicating that stresses are almost equally distributed (Karami and Shankar, [1]).

3.4. Verification Of The Tissue Response With Experimental Data

Experimental results obtained by Velardi et al. (4) for different porcine brain samples are in two forms (a) axonal fibers are oriented in longitudinal direction (b) axonal fibers oriented in a transverse direction within the white matter sheet corona radiate (Karami and Shankar, [1]).

In the computational analysis, loads created due to displacements in load case 1 and load case 2 with different axon volume fractions (40%, 53% and 60%) are applied and the results for average volume normal stresses developed in the brain tissue are verified experimentally as shown in figures 16 and 17.

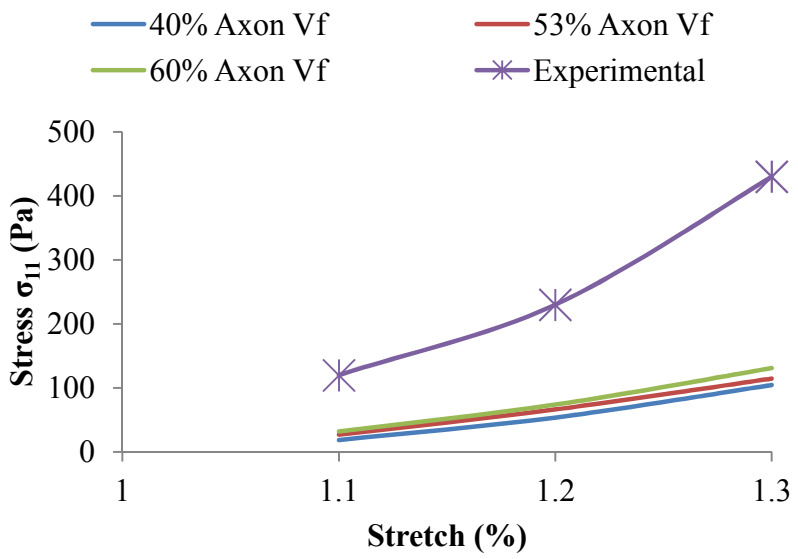

Fig 32. Load case 1. S11 Average Normal stresses in Corona radiata for volume fractions 40%, 53%, 60% and experimental (Levenberg-Marquardt nonlinear fit method [5]) (Karami and Shankar, [1]).

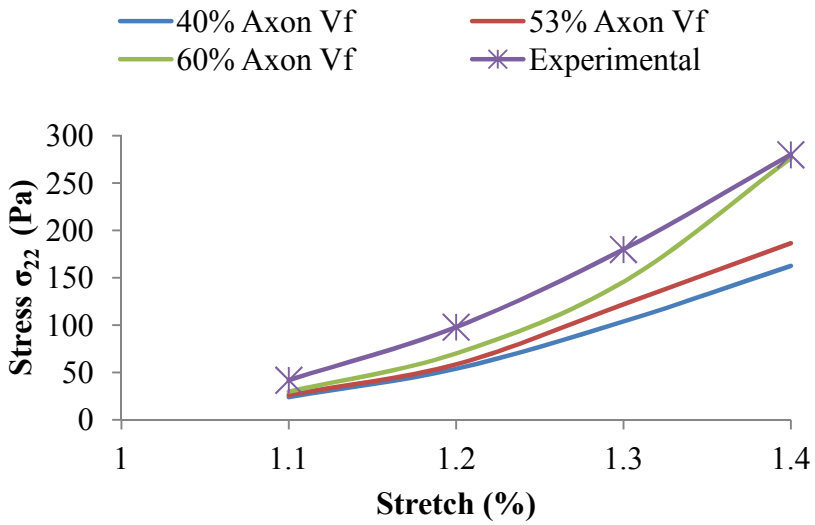

Fig 33. Load case 2. S22 Average Normal stresses in Corona radiata for volume fractions 40%, 53%, 60% and experimental (Levenberg-Marquardt nonlinear fit method [5]) (Karami and Shankar, [1]).

Arbogast and Margulies [6] reported that for uniaxial orientation of axons within the white matter sheet corpus collasum, the ideal axonal volume fraction is 53% (Karami and Shankar, [1]). In case of bi-directional orientation of axonal fibers in corona radiate, results were different (Karami and Shankar, [1]). For load case 1, where the loads created due to displacements are applied in longitudinal direction, the computational results were not in agreement with the experimental data (Karami and Shankar, [1]). While for load case 2, where loads are applied in transverse direction, the results for 60% axonal volume fraction are in close proximity with the experimental data available (Karami and Shankar, [1]).

4. CONCLUSIONS AND SUGGESTIONS FOR FUTURE WORK

Characterization of brain white matter sheet *corona radiata* consisting of axons oriented in a bi-directional pattern within extracellular matrix is done by making a three dimensional micromechanical model representing a unit cell. Various axon volume fractions (40%, 53% and 60%) are taken into account and for each respective volume fraction; deformation occurring within the axons by applying loads are shown which depicts that how Diffuse Axonal Injury occurs when a fast moving object penetrates through the skull into the human brain (Karami and Shankar, [1]). Axial and shear loads were applied on the unit cells to understand the behavior of the brain tissue (Karami and Shankar, [1]). For the different loads applied in the longitudinal direction and transverse direction axial stresses were almost evenly distributed but not for the case of shear stresses.

Modeling the unit cells with different axon volume fractions creates an effect on the properties of white matter brain tissue *corona radiata* (Karami and Shankar, [1]). As the axonal volume fraction increases, the maximum normal stresses developed in the *corona radiata* increases for each stretch value considered (Karami and Shankar, [1]).

The computational results were compared with the experimental results. It can be concluded that when the loads were applied in longitudinal direction the results were slightly conflicting but for loads in transverse direction, the results were in correlation with the experimental data (Karami and Shankar, [1]). For Load case 2, it can be inferred that for bi-directional orientation of axon fibers, the ideal volume fraction of axons can be near to 60% (Karami and Shankar, [1]). While for load case 1, it might be that axon volume fraction be different with that considered for load case 2 (Karami and Shankar, [1]). The angle at which the axons are inclined also plays an important role in finding out the ideal axon volume fraction for bi-direction orientation of fibers.

In this present study, the axons were oriented at right angle to each other. Models should be developed at different angles and hence the computational results must be verified experimentally.

The experiment on brain tissue for shear loading should also be done and verified computationally (Karami and Shankar, [1]). The material properties of the brain tissue constituents provided are not sufficient. The model provided must be refined in order to obtain more accurate results by considering bi-directional crossed axonal fibers at different angles (Karami and Shankar, [1]).

The bidirectional orientation of axonal fibers as compared to uni-directional arrangement of axons within the white matter sheet of brain tissue is less explored and hence more works needs to be done in this area (Karami and Shankar, [1]). The model provided can be further used for micromechanical characterization of brain white matter when accurate experimental results as well as precise material properties of axonal fibers and base matrix are obtained (Karami and Shankar, [1]).

REFERENCES

[1] Karami G. and Shankar S., A mutiscale analysis of the white brain material with axons as bidirectional oriented fibers, 2011 SIMULIA Customer Conference, 1-14.

[2] ABAQUS. 2006. User's Manual, Version 6.6, Providence, RI: Hibbit, Karlsson and Sorensen, Inc.

[3] Rhawn Joseph, Ph.D. Neuropsychiatry, Neuropsychology, Clinical Neuroscience. Head Injuries: Cerebral and Cranial Trauma Skull Fractures, Concussions, Contusions, Hemorrhage, Loss of Consciousness, Coma. Lecture - Chapter 11

[4] Wolf J.A., Stys P.K., Lusardi T., Meaney D., and Smith, D.H. (2001). Traumatic axonal injury induces calcium influx modulated by tetrodotoxin-sensitive sodium channels. Journal of Neuroscience. 21 (6): 1923–1930.

[5] Velardi, F., Fraternali, F., and Angelillo, M., 2006. Anisotropic constitutive equations and experimental tensile behavior of brain tissue. Biomech. Model Mechanobiol. 5, 53-61.

[6] Arbogast, K.B., Margulies, S.S., 1999. A fiber-reinforced composite model of the viscoelastic behavior of the brainstem in shear. *Journal of Biomechanics,* Volume 32, Issue 8, Pages 865-870.

[7] Abolfathi, N., Naik, A., Karami, G., Ulven, C., 2008. "A micromechanical characterization of angular bidirectional fibrous composites", Computational Materials Science. Volume 43, Issue 4, October 2008, Pages 1193-1206.

[8] Karami, G., Grundman, N., Abofathi, N., Naik, A., Ziejewski, M., 2009. A micromechanical hyperelastic modeling of brain white matter under large deformation. Journal of the Mechanical Behavior of Biomedical Materials Volume 2, Issue 3, July 2009, Pages 243-254.

[9] Prange, M.T., Margulies, S.S., 2002. Regional, directional, and age dependent properties of the brain undergoing large deformation. J. Biomech. Eng. 124, 244-252.

[10] Ogden RW (2003). Nonlinear Elasticity, Anisotropy, Material Stability and Residual Stresses in Soft Tissue. Biomechanics of Soft Tissue in Cardiovascular Systems. CISM Courses and Lectures Series no. 441, pp. 65-108(Springer, Wien, 2003: ISBN 3-211-00455-6).

[11] Bhatti, M.A., 2006. Advance Topics in Finite Element Analysis of Structures. John Wiley &Sons, Inc., New York.

[12] Meaney, D.F., 2003. Relationship between structural modeling and hyperelastic material behavior: Application to CNS white matter. Biomech Model Mechanobiol. 1, 279-293.

[13] Spencer AJM (1984). Constitutive theory for strongly anisotropic solids. In Spencer, A.J.M., ed., Continuum theory of the mechanics of fiber-reinforced composites. Wien: Springer-Verlag. CISM Courses and Lectures, No. 282. Springer-Verlag, Wien,pp : 1-32.

[14] Holzapfel,G.A.(2000). Nonlinear Solid Mechanics. Wiley, Chichester.

[15] Aboudi, J. (1991). Mechanics of Composite Materials, A unified micromechanical approach, *Elsevier Science Publishers, Amsterdam*.

[16] Needleman, A. and Tvergaard, V. (1993). Comparison of crustal plasticity and isotropic hardening predictions of metal-matrix composites, *ASME Journal of Applied Mechanics, 60*, 70-76.

[17] Hashin, Z. and Rosen, B.W. (1964). The elastic moduli of fiber-reinforced materials, *ASME Journal of Applied Mechanics, 31*, 223-232.

[18] Hashin, Z. (1972). Theory of Composite Materials, NASA Contractor Report, CR-1974.

[19] Hashin, Z. (1983). Analysis of composite materials- a survey, *Journal of Applied Mechanics, 105*, 481-504.

[20] Xia, Z., Chen, Y. and Ellyin, F. (2000). A meso/micro-mechanical model for damage progression in glass-fiber/epoxy cross-ply laminates by finite-element analysis, *Composite Science and Technology*, 60, 1171-1179.

[21] Chen, Y., Xia, Z. and Ellyin, F. (2001). Evolution of residual stresses induced during curing processing using a viscoelastic micro-mechanical model, *Journal of Composite Materials, 3*5, 522-542.

[22] Garnich M, Karami G. 2004. Finite element micromechanics for stiffness and strength of wavy fiber composites. *Journal of Composite Materials*. 38(4): 273-292.

[23] Karami G, Garnich M. 2005a. Effective moduli and failure considerations for composite with periodic fiber waviness. *Journal of Composite Structures. 67*: 461-475.

[24] Naik A, Abolfathi N, Karami G, Ziejewski M. 2008. Micromechanical viscoelastic characterization of fibrous composites. *Journal of Composites Materials. 42*: 1179-1204.

[25] Snedeker, J.G., Niederer, M., Schnidlin, P., Farshad, F.R., Dametropoulos, C.K., Lee, J.B., Yang, K.H., 2005b. Strain rate dependent material properties of the porcine and human kidney capsule. *Journal of Biomechanics 3*8, 1011-1021.

[26] Snedeker, J.G., Barbezat, M., Niederer, P., P., Schnidlin, F.R Farshad, M., 2005a. Strain energy density as a rupture criterion for the kidney; impact test on porcine organs, finite element simulation, and a baseline comparison between human and porcine tissues. *Journal of Biomechanics* 38, 993-1001.

[27] Miller, K., Chinzei, K., 1997. Constitutivr modeling of brain tissue: experiment and theory. Journal of Biomechanics 30, 1115-1121.

[28] Arbogast, K.B., Thibault, K.L., Pinheiro, S., Winey, K.I., Margulies, S.S., 1997. A high frequency shear device for testing soft biological tissues. *Journal of Biomechanics 30*, 757-759.

[29] Abolfathi, N., Naik, A., Sotudeh, M., Karami, G. and Ziejewski, M. (2009). A micromechanical procedure for characterization of the mechanical properties of brain white matter, Computer Methods in Biomechanics and Biomedical Engineering, 12(3), 249-262.